Showcasing research from Professor Prasanth Raghavan's group, Materials Science and NanoEngineering Lab (MSNE-Lab), Cochin University of Science and Technology (CUSAT), India and Professor Alexandru Vlad's Laboratory, Université Catholique de Louvain, Belgium.

Recent advances in electrospun fibers based on transition metal oxides for supercapacitor applications: a review

The review article unveils the fundamentals of the electrospinning technique, detailed insight into the advantages and disadvantages of fiber supercapacitors with latest advancement in transition metal oxide based electrospun fiber electrodes along with its challenges and future prospects for sustainable supercapacitor applications. Cover art conceptualized and designed by MSNE-Lab, CUSAT.

As featured in:

See Sivaramapanicker Sreejith, Prasanth Raghavan *et al.*, *Energy Adv.*, 2023, **2**, 922.

ROYAL SOCIETY OF CHEMISTRY

rsc.li/energy-advances

REVIEW ARTICLE

Check for updates

Recent advances in electrospun fibers based on transition metal oxides for supercapacitor applications: a review

Abhilash Pullanchiyodan, [a] Roshny Joy,[a] Pranav Sreeram,[a] Leya Rose Raphael,[a] Akhila Das,[a] Neethu T. M. Balakrishnan,[a] Jou-Hyon Ahn, [b] Alexandru Vlad, [c] Sivaramapanicker Sreejith [*a] and Prasanth Raghavan [*abd]

Recent critical advances in energy storage technologies and progress towards the future "electric" era highlight the enormous demand for sustainable energy storage devices like batteries and supercapacitors (SCs) to meet the acute energy needs of society. SCs are more remarkable among the various technologies due to their high power density, extended life cycle, environmental friendliness, and fast charging–discharging. To further improve the performance of SC devices, tremendous research efforts are in progress, including altering the fabrication method, using advanced robust materials and intriguing engineered nanostructures, and designing new architectures. Among the widely available materials, transition metal oxides (TMOs) exhibit good performance in SC technology owing to their high specific capacitance, different oxidation states, chemical and thermal stability and economic viability. So, recent research focuses on developing multifunctional engineered nanostructures and composites of TMOs to improve the SC performance and widen their application towards wearable and healthcare devices. The nanofiber morphology is supposed to have several advantages in SC performance compared to other morphologies owing to its higher specific surface area and aspect ratio, effectively improving the adsorption and electrolyte-ion diffusion process. Electrospinning is the most efficient technique for large-scale nanofiber production in a facile approach. This review discusses the recent progress in the fabrication and electrochemical properties of various TMO-based electrospun fiber electrodes for SC applications. The fundamentals of the electrospinning technique and a basic overview, in addition to the classification of SCs, are summarised. A more detailed insight into the advantages and disadvantages of fiber SCs, with particular attention on electrospun TMO fibers, is also discussed in this review. Finally, a conclusion on different TMO-based electrospun fiber electrodes compared to bimetal TMOs is deliberated by stating the challenges and future prospects of electrospun fiber SC electrodes.

Introduction

The depletion of fossil fuel-based energy sources and the ever-increasing demand for daily energy consumption has accelerated the need for alternative and sustainable energy sources.[1–8]

[a] Materials Science and NanoEngineering Lab (MSNE-Lab), Department of Polymer Science and Rubber Technology (PSRT), Cochin University of Science and Technology (CUSAT), Cochin 682022, India. E-mail: prasanth@cusat.ac.in, praghavan@sruc.ac.uk, sreejith.siva@gmail.com; Tel: +91-(0)-790 753 3273, +44-7385848398

[b] Department of Materials Engineering and Convergence Technology, Gyeongsang National University, 501 Jinju-daero, Jinju 52828, Republic of Korea

[c] Institute of Condensed Matter and Nanosciences, Université Catholique de Louvain, 1348 Ottignies-Louvain-la-Neuve, Belgium

[d] Biorefining and Advanced Materials Research Centre, Scotland's Rural College (SRUC), Kings Buildings, West Mains Road, Edinburgh, EH9 3JG, UK

Besides, fossil fuel combustion also results in atmospheric pollution through the emission of toxic and greenhouse gases.[2,4,9–11] Safe and viable energy storing devices have attracted prominent interest in this regard. The discovery of the possibility of storing charges on the surface has created historic innovations in the energy storage sectors.[12] Electrochemical energy storage (EES) devices such as batteries, supercapacitors (SCs) and fuel cells are some of the most important classes of sustainable and renewable energy storage techniques nowadays.[13–22] Even though some fundamental differences exist in the operation of these three techniques, some electrochemical similarities persist. The energy storing process of these devices takes place in the electrode–electrolyte interface and has a separate path for electron and ion transport.[13,23] Moreover, in their architecture, these EES devices are made up of two electrodes separated by an electrolyte. Fig. 1(a)

shows the Ragone plot of the energy and power densities of different charge-storing devices, including batteries, SCs and fuel cells.[24]

SCs have attracted much more scientific and technological care owing to their environmental friendliness, safety, high power density and better cycling stability than other electrochemical energy storing devices.[25–34] However, comparatively, the low energy density of SC is the main disadvantage, which hinders the widespread application of SCs.[35–39] In order to address this challenge, different materials and methods are utilized in SC technology. A more detailed discussion on SCs and their primary classifications and working mechanisms are given in the following sections (Fig. 1(b)–(d)).[40] Carbonaceous materials, transition metal oxides (TMOs), two-dimensional (2D) materials, conducting polymers and nanocomposites are the most extensively used electrode materials in SCs.[27,29,41,42] Among these, the transition metal oxides have promising results in attaining high specific capacitance and better energy density.[6,43,44] Yet, their low electrical conductivity is one of the main weaknesses, and the fabrication of TMO nanocomposites with conductive carbon nanomaterials like graphene, carbon nanotubes (CNTs), and carbon fibers aids in increasing the electrical conductivity and better capacitive performance.[43,45–48] Among the different techniques, electrospinning is the cheapest and most widely used technique to make carbon nanofibers having better porosity and high specific surface area.[49,50]

Hence, in this review, we focus on the role of electrospun nanofiber electrodes with transition metal oxide additives in the performance of fiber supercapacitors. A brief overview of the fundamentals of electrospinning, supercapacitors and their different classifications based on storage mechanisms and recent advances in fiber supercapacitors are included in this review. The role of transition metal oxides in supercapacitor electrode fabrications, followed by a detailed review of electrospun transition metal oxides for fiber supercapacitors is included in the final section of the review.

Fundamentals of electrospinning

Electrospinning is a technique that Lord Rayleigh developed for fabricating fiber structures by exploiting the electrostatic force.[51] Compared to other processing techniques, electrospinning's main benefit is the large-scale nanofiber production in a facile and highly versatile approach.[51,52] There are different reviews available explaining the basic mechanism of the electrospinning process and different processing parameters and conditions that affect the electrospinning process.[53–56] In this regard, we give a brief overview of the electrospinning process. As shown in Fig. 2(a), the basic components of an electrospinning unit are a high voltage power supply, spinning unit (syringe and pump) and grounded collector.[57,58] During the

Abhilash Pullanchiyodan

Dr Abhilash Pullanchiyodan is a Chief Minister's Nava Kerala Postdoctoral Fellow (CMNPF) at the Materials Science and NanoEngineering Lab (MSNE-Lab), Department of Polymer Science and Rubber Technology (PSRT), Cochin University of Science and Technology (CUSAT), India. He received a BSc and MSc degree in Chemistry, from Kannur University, India, and PhD degree in Chemical Science (Chemistry) in 2018, from Academy of Scientific and Innovative Research (AcSIR), India. From 2018 he worked as a Post-doctoral fellow/Research staff at University of Glasgow, UK, and later he was awarded the prestigious Royal Society-SERB Newton International Fellowship in 2019. He has also worked as a postdoctoral fellow at National Institute of Technology (NITK), Surathkal, India. He is the recipient of a CSIR-SRF fellowship. His research interests include supercapacitors, batteries, 2D materials, nanomaterial and polymer composites, ink/paste formulations, microwave dielectrics and ceramics. Dr Abhilash has published more than 35 peer reviewed research articles in high impact factor journals and a number of books/book chapters, and has over 900 citations and an h-index of 17.

Roshny Joy

Roshny Joy is a Senior Research Fellow (SRF) at Materials Science and NanoEngineering Lab (MSNE-Lab), Department of Polymer Science and Rubber Technology (PSRT), Cochin University of Science and Technology (CUSAT), India. Her current research is focused on high voltage window flexible super capacitors under the guidance of Prof. Prasanth Raghavan. She received her BSc degree from Mahatma Gandhi University, Kerala and MSc degree in Chemistry from Malaviya National Institute of Technology (MNIT), Rajasthan. She completed her MPhil degree at CUSAT. Her current areas of interest include supercapacitors, 2D materials, nanomaterials and composites and flexible energy storage devices.

process, a high DC voltage is applied between the collector and spinneret, which will be responsible for forming a Taylor cone

of the spinning solution at the tip of the needle. The Taylor cone will elongate into the collector as a fiber mat when the

Pranav Sreeram

Pranav Sreeram is a budding scientist who joined as a graduate student at Department of Polymer Science and Rubber Technology (PSRT), Cochin University of Science and Technology (CUSAT), Cochin, India in the year 2020. Later he started to work with Prof. Prasanth Raghavn at Materials Science and NanoEngineering Lab (MSNE-Lab) @PSRT from spring 2022. He is working in the research area of the production of nanocellulose and self-assembled lignin nanocrystals from animal manure as a sustainable material for energy harvesting and storage applications. Sreeram is actively involved in the development of flexible solid state polymer electrolytes or quasi solid electrolytes for batteries and supercapacitors. He has keen research interest in nanomaterials, energy harvesting and storage devices, sustainable materials and bio plastics. He has authored a couple of peer reviewed scientific articles or book chapters with leading international academic publishers. He has also been a visiting intern at Mishra's Research Lab, at Birla Institute of Technology (BIT), Ranchi, India since 2022, and is collaboratively working with Prof. Vijay Kumar Thakur at Biorefining and Advanced Materials Research Centre, Scotland's Rural College, University of Edinburgh, UK on extraction and modification of nanocellulose from Hemp and animal manure for supercapacitor applications.

Leya Rose Raphael

Leya Rose Raphael received her MSc degree in Applied Chemistry (Oils, Fats and Aromatics) after receiving her BSc degree in Chemistry from Mahatma Gandhi University, Kottayam and is currently pursuing a PhD at the Material Science and NanoEngineering Laboratory (MSNE-Lab), Department of Polymer Science and Rubber Technology, Cochin University of Science and Technology. She has expertise in the synthesis and characterization of conducting polymers, graphene/2D materials and superhydrophobic membranes. Currently a Senior Research Fellow (SRF), her research work focuses on the development of tailor made 3D Cob-web Nano fibrous electrolytes for high-temperature Li-ion batteries as well as environmental applications. Several book chapters with International Publishers are in her credits.

Akhila Das

Akhila Das is a graduate student pursuing a PhD at Materials Science and NanoEngineering Laboratory (MSNE-Lab), Department of Polymer Science and Rubber Technology (PSRT), Cochin University of Science and Technology, India. Her research area is focused on the "Development of alternative batteries other than Li-ion technology" with special interest in sodium ion batteries and magnesium ion batteries and the fabrication of flexible and bendable all solid state supercapacitors having high voltage window. More than 35 peer reviewed international publications and a good number of international conference proceedings are to her credit. She is the author of a two volume set reference book entitled "New trends in rechargeable batteries-the advanced energy storage solutions" published by Taylor & Francis, CRC Press, USA. Her current area of interest includes batteries, supercapacitors and e-waste management for a sustainable future and a green environment.

Neethu T. M. Balakrishnan

Neethu T. M. Balakrishnan is pursuing her PhD thesis with Prof. Prasanth Raghavan, at Material Science and NanoEngineering Laboratory (MSNE-Lab), Department of Polymer Science and Rubber Technology, Cochin University of Science and Technology (CUSAT), India. Currently, she is working in the field of energy harvesting and storage devices. Her research work is focused on the development of polymer membrane-based tribo electric nanogenerators and safe electrolytes for heavy duty lithium ion batteries. More than 35 peer reviewed international publications and a good number of international conference proceedings are to her credit. She is the author of the book entitled 'Electrospinning for Advance Energy Storage Applications' on lithium-ion batteries. Her current areas of interest include electrospinning, carbon nanomaterials, ceramics, metal oxides, flexible and bendable energy harvesting and storage solutions such as triboelectric nanogenerators, lithium-ion batteries and supercapacitors.

solution overcomes the electrostatic force.[58] As aforementioned, the properties of the fiber can be controlled and tuned by varying some of the spinning factors, like (i) system parameters (molecular weight and molecular weight distribution polymer chain, linear or branched chain architecture of the polymer, *etc.*), (ii) solution parameters (concentration, viscosity, surface tension and dielectric constant), (iii) process parameters (applied voltage, rotation speed, feeding rate, collector type, tip and collector gap), and (iv) ambient conditions (humidity, temperature and air velocity in the chamber).[51,58] Each of these parameters has a different extent of influence on the spinning process, and among these, the solution process plays a pivotal role in determining the quality of the spun fiber mat. For example, a low viscosity of the spinning solution can result in bead formation on the spun fiber mat, whereas a higher viscosity can lead to increased fiber diameter. Hence, the tunable properties of the electrospinning fiber give more opportunities to manipulate the electrode properties for better performance.[59] Likewise, the geometry (static: plate collector or screw jacks and dynamic: rotating drum) and type of collector material (aluminium foil, copper foil, wire mesh, conductive cloth and carbon paper) have a huge impact in controlling the fiber morphologies from random fibers to aligned/intertwined fibers and their physical properties (Fig. 2(b)).[60] Fig. 2(c) represents the morphological variation of fibers collected using different collectors.[61,62] Another important aspect of electrospinning techniques is that, rather than the basic polymeric solution for spinning, various additives like metals, metal oxides and nanoparticles can be incorporated into the spinning solution, which further allows the properties of the spun fibers to be manipulated.[49,63–66] Fig. 2(d) shows the schematic representation of different parameters, which influences the electrospinning process.[67,68]

Supercapacitors (SCs)

As aforementioned, supercapacitors are a class of electrochemical energy storage device with interesting characteristics, such as high power density, low charging–discharging time, high cyclic stability, environmental friendliness, flexibility and ease of integration.[12,13,26,69–71] Thanks are due to material science and technology, which helped to improve the low energy density of the SC to a greater extent through the tremendous development that happened in materials sectors and design aspects.[72] Based on the mechanism of charge storage, the SCs can be broadly classified into three different categories, namely (i) electrochemical double-layer capacitors, (ii) pseudocapacitors and (iii) hybrid capacitors.[10] A schematic representation of these classifications and an overview of the different electrode materials used in these SCs are shown in Fig. 1(b).[42,73]

Classification of supercapacitors

Electrochemical double-layer capacitors (EDLCs). The basic working principle of charge storage in EDLCs is based on the reversible adsorption of ions in the electrolyte on a high surface area electrode material and hence the generation of electrostatic charge on the surface of the electrode.[42,74] The carbon-based materials are the most commonly used electrode materials for EDLCs, including carbon nanotubes (CNTs), graphene and activated carbon, *etc.*[74] The device's capacitance is calculated using the famous Helmholtz equation below.

$$C = \frac{\varepsilon_0 \varepsilon_r A}{d}$$

where 'ε_0' and 'ε_r' are the dielectric constant of the vacuum and electrolyte, respectively, 'A' is the electrode surface area, and 'd' is

Jou-Hyon Ahn

Prof. Jou-Hyeon Ahn is a professor in Department of Materials Engineering and Convergence Technology, Gyeongsang National University (GNU), Republic of Korea. He received his MS and PhD degree from Department of Chemical Engineering, Korea Advanced Institute of Science and Technology (KAIST), Republic of Korea. His research interest is mainly focused on high energy density next generation batteries including lithium sulfur and sodium sulfur batteries. He has published about 400 scientific articles having citations of about 11500 and an h-index of 60. Prof. Ahn has been indexed as a top 2% scientist in the world by Stanford University, USA in the last couple of years and also listed in the top ranked world scientists by AD Scientific. He sits on the editorial board of a couple of SCI international journals as an Editor or Editorial Advisory Board member.

Alexandru Vlad

Prof. Alexandru Vlad is an Assistance professor in chemistry of Division of Molecular Chemistry, Materials and Catalysis, Institute of Condensed Matter and Nanoscience, University catholique de Louvain. He received his PhD in Applied Sciences, in 2009, Université catholique de Louvain, and Belgium. His research has primarily focus on the design and synthesis of materials and architectures to address the new challenges arising in the field of electrochemical energy storage and conversion. He was awarded an ERC Grant (MOOiRE, GA 770870) I 2017, and his major expertise were consolidated on organic and organometallic chemistries and materials for energy storage, including high-voltage organic battery materials. He has more than 3500 citations and an h-index of 35.

the charge separation distance or effective thickness of the double layer.[74]

The interesting factor of EDLCs is that the rate of formation and relaxation of the electric double layer at the electrode surface is very high (almost on the order of 10^{-8} S), so this will respond very rapidly to potential change and doesn't involve any chemical reaction, rather only a charge rearrangement.[13] Due to this phenomenon, EDLCs show very high cycling stability (more than 10^6 cycles) and a low rate of material degradation. However, one of the main drawbacks of EDLCs is their low energy density.

Pseudocapacitors

Unlike EDLCs, in pseudocapacitors, the mechanism of charge storage is primarily centred on a reversible faradaic redox reaction on the electrode material's surface.[74] This redox reaction leads to an increased capacitance and, thereby an improvement in energy density compared to EDLCs. Mainly transition metal oxides like MnO_2 and RuO_2 are used as the pseudocapacitive electrode material.[74] Rather than metal oxides, conducting polymers (like polyaniline, polypyrrole, PEDOT:PSS and polythiophene) and metal-doped carbons are also used as pseudocapacitive materials.[69,74] Compared to a battery, the redox reaction mainly occurs on the surface or near the surface volume of the electrode. Besides this, the distinctive features of pseudocapacitive electrodes are (i) they have a charge which varies with potential, (ii) surface pseudocapacitance (the absence of a solid-state diffusion limitation) and (iii) the lack of phase change in electrochemical reaction.[75] Even though the pseudocapacitive materials have high specific capacitance and energy density, their use in commercial applications is some-

Prasanth Raghavan

Prof. Prasanth Raghavan is a Professor and Head of the department at the Department of Polymer Science and Rubber Technology (PSRT), Cochin University of Science and Technology (CUSAT), India, and Visiting Professor at Gyeongsang National University, Republic of Korea and Scotland's Rural College (SRUC), University of Edinburgh, UK. Prof. Prasanth is also holding the Associate/Adjunct Faculty position at the InterUniversity Centre for Nanomaterials and Devices (IUCND), CUSAT. He was indexed as a top 2% scientist in the world by Stanford University, USA in last couple of years. He received his PhD in Engineering under the guidance of Prof. Jou-Hyeon Ahn, from the Department of Chemical and Biological Engineering, Geyongsang National University, Republic of Korea, in 2009, supported by a prestigious Brain Korea (BK21) Fellowship. Prof. Prasanth completed his B. Tech and M. Tech from CUSAT. After a couple of years of attachment as a Project Scientist at the Indian Institute of Technology (IIT-D), New Delhi, he moved to the Republic of Korea for his PhD studies in 2007. His PhD research was focused on the fabrication and investigation of nanoscale fibrous electrolytes for high-performance energy storage devices. After his PhD, Prof. Prasanth joined Nanyang Technological University (NTU), Singapore, as a Research Scientist, in collaboration with the Energy Research Institute at NTU (ERI@N) and TUM CREATE, a joint electromobility research centre between Germany's Technische Universität München (TUM) and NTU, where he was working with Prof. (Dr) Rachid Yazami, who successfully introduced graphitic carbon as an anode for commercial lithium-ion batteries, and received the Draper Prize in 2014. After four years in Singapore, Prof. Prasanth moved to Rice University, USA as a Research Scientist, where he worked with Prof. (Dr) Pulickal M Ajayan, the co-inventor of carbon nanotubes, and was fortunate to work with 2019 Chemistry Nobel Prize laureate, Prof. (Dr) John B. Goodenough. Prof. Prasanth was selected for the Brain Korea Fellowship (2007), SAGE Research Foundation Fellowship, Brazil (2009), Estonian Science Foundation Fellowship, European Science Foundation Fellowship (2010), Faculty Recharge, University Grants Commission (UGC), Ministry of Higher Education, India (2015), etc. Prof. Prasanth has received many international awards, including the Young Scientist award, Korean Electrochemical Society (2009), and was selected for the Bharat Vikas Yuva Ratna Award (2016) and recently awarded with an Education Excellence Award (2021), Dr S Radha krishnan Bharat Shiksha National Award (2021) etc. His current research focuses on nanoscale materials and polymer composites for printed and lightweight charge storage solutions, including high-temperature supercapacitors, batteries and tribo electric nanogenerators. Prof. Prasanth has published many research papers in high-impact factor journals, and a number of books/book chapters, and has around 7000 citation and an h-index of 40 plus. He sits on the editorial board as an Editor or Editorial Advisory Board member of SCI international journals including Journal of Materials Research, Nanofabrication, Biomaterials and Polymers Horizon and Frontiers of Materials etc. Prof. Prasanth is a book series editor for Springer Nature, Elsevier, Taylor and Francis, CRC Press etc. Apart from science and technology, Prof. Prasanth is a poet, activist and columnist in online portals and printed media.

Sivaramapanicker Sreejith

Sivaramapanicker Sreejith is currently visiting faculty at the Materials Science and Nanoengineering Lab (MSNE-Lab), Cochin University of Science and Technology, Kerala, India. He obtained his PhD in Chemistry from the CSIR-National Institute for Interdisciplinary Science and Technology (CSIR-NIIST), INDIA in 2010. Subsequently, he became an Alexander von Humboldt Fellow (2010–2011) at Humboldt University, Germany. He then moved to Nanyang Technological University, Singapore (2011–2017). Later in 2017, he moved to National University of Singapore (NUS), Singapore (2017–2019) as a Senior Research Fellow at the Institute for Health Innovation and Technology-NUS, Singapore. His research interest includes the study of functional nanomaterials, hybrids and nanocomposites with a focus on their applications in biological, catalytic and energy systems. He has published more than 65 scientific articles (4600 citations, h-index-29) in leading peer reviewed journals and has contributed to several book chapters.
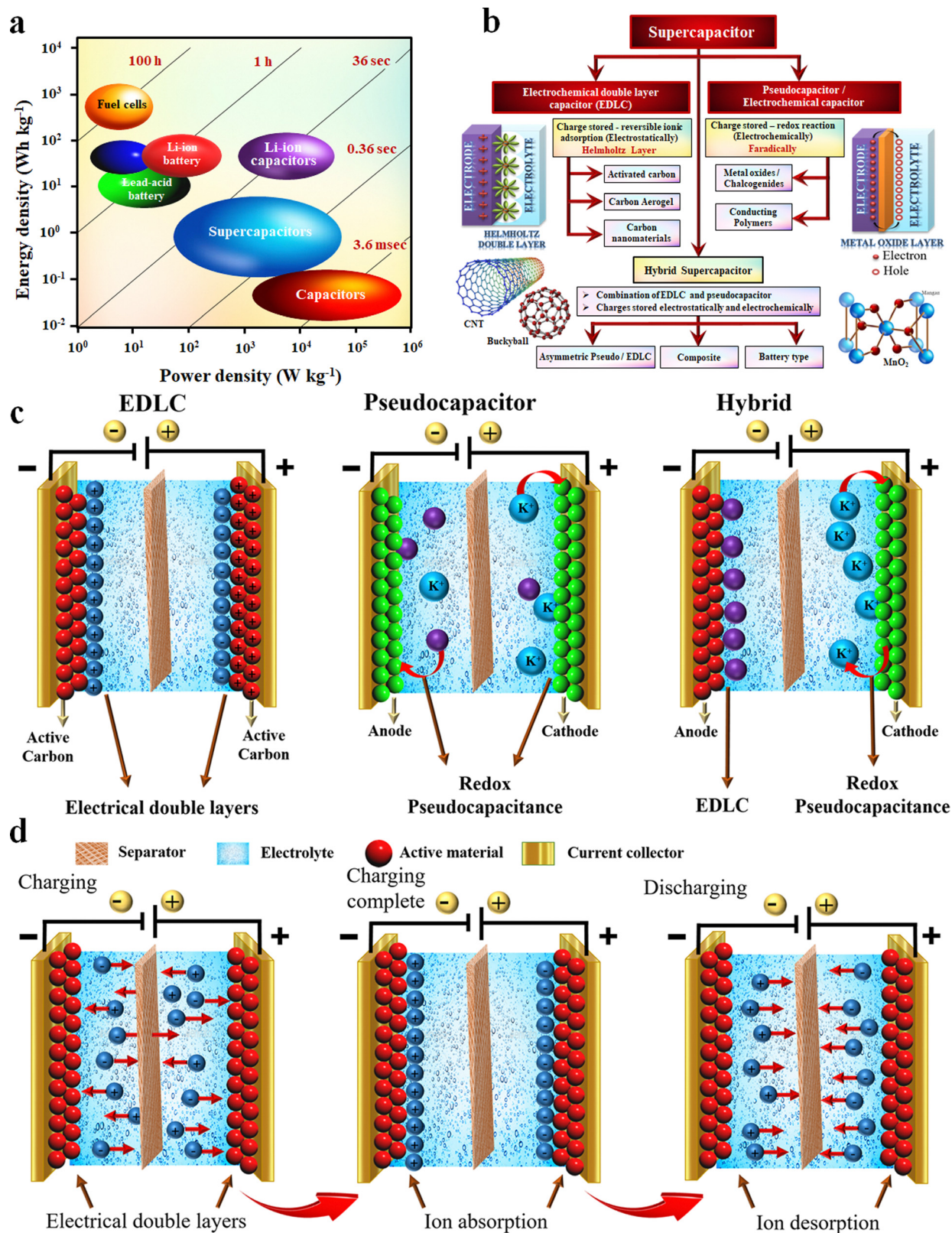
Fig. 1 (a) Ragone plot. Reproduced from ref. 24 with permission from Wiley, copyright 2015. (b) Classification of SCs and (c and d) working mechanism of SCs. Reproduced from ref. 40 with permission from Springer, copyright 2022.

Fig. 2 (a) Basic instrumentation. Reproduced from ref. 57 with permission from Springer, copyright 2021. (b) Different types of collectors. Reproduced from ref. 60 with permission from Springer, copyright 2016. (c) Microstructure of various alignments of fiber with different types of collectors in electrospinning. Reproduced from ref. 61 and 62 with permission from Elsevier, copyright 2015, Royal Society of Chemistry, copyright 2017. (d) Factors affecting electrospinning technique.

how limited due to the high cost (RuO_2), low electrical conductivity (MnO_2 and other metal oxides), and low cycling stability of the polymer-based materials.[75]

Hybrid supercapacitors

Hybrid SCs contain both faradaic (pseudocapacitive) and non-faradaic or carbon-based (EDLC) electrodes in their design. Hence, the battery and capacitor-type electrodes in a single hybrid device show enhanced capacitance, high energy density and better cycling stability. Based on the electrode materials and configuration used in hybrid SC fabrication, they can be further classified into the following categories.[42]

Asymmetric supercapacitors

Asymmetric SCs consist of two dissimilar electrodes in which carbon-based materials (EDLC) will be used as the negative electrode, and metal oxides or conducting polymers (pseudo) will serve as the positive electrode of the device.[42]

Composite supercapacitors

In composite electrodes, the single electrode will consist of carbon and pseudocapacitive materials in binary or ternary composite form. The synergetic contribution from both materials (EDLC and pseudocapacitance) is responsible for the enhanced performance in a composite electrode.[42]

Battery-type supercapacitors

Battery-type supercapacitors are similar to asymmetric ones, but the electrode should be made of battery-type materials. This configuration type motivates the utilization of both battery and supercapacitor-type performance in a single device.[42]

Fiber supercapacitors

Wearable electronics, including healthcare monitoring devices, biomedical devices, sports wares, flexible displays and sensors, are getting broader consideration in recent years owing to their better technological and industrial advantages.[26,69] These rapid enhancements in wearable electronics have accelerated the need for wearable energy storage devices that are ultra-flexible, lightweight, and can be easily integrated with wearable gadgets.[26,69] Herein, flexible supercapacitors (FSCs) are suitable candidates for such applications owing to their better stability and nontoxic nature. The mechanical stability of these SCs is crucial for wearable applications. Hence a one-dimensional (1D) fiber-based SC having a length in millimetres and a diameter of a few micrometres is a suitable choice.[76] The advantages of FSCs over other conventional SCs are (i) higher mechanical flexibility, (ii) ease of scale up and (iii) space and shape compatibility.[76] The first work on fiber SCs was reported in 2003 by Baughman et al., demonstrating a CNT-based FSC integrated into textiles.[76,77] Thereafter, many reports have become available on FSCs, including some of the pioneering work from Wang et al. using the pseudocapacitive ZnO and MnO_2 for FSC fabrication.[76,78] The roadmap of FSC growth is represented schematically in Fig. 3(a).

Fig. 3 (a) Chronological growth of FSCs. Reproduced from ref. 76 with permission from Wiley, copyright 2020. (b) No. of publications on MnO$_2$/carbon composites for SC electrodes. (c) Different types of carbon materials used for SC electrode fabrication with MnO$_2$. Reproduced from ref. 88 with permission from Frontiers, copyright 2020. (d) Comparison of theoretical specific capacitance of different TMOs. Reproduced from ref. 84 with permission from Elsevier, copyright 2020.

Nanofibers for SC fabrications

The major criteria for selecting electrode materials for better performance include high specific surface area, better electronic/ionic conductivity and better chemical stability.[79] The high surface area of the electrode material is so important since most of the electrochemical reactions take place on the surface of the electrode.[79] In this regard, using nanostructured materials will help to enhance the electrode material's specific surface area. Based on the aspect ratios, the nanostructures are broadly classified into zero-dimensional (0D, *e.g.* quantum dots), one-dimensional (1D, *e.g.* nanofiber, nanowires, nanotubes), two-dimensional (2D, *e.g.* nanosheets) and three-dimensional (3D, *e.g.* mesoporous graphene or carbon aerogels) nanomaterials.[79]

The 1D nanomaterials, especially nanofibers, show better performance in electronic and energy storage applications due to their favourable length, which allows unrestricted free flow of electrons resulting in efficient energy transport.[76] Similarly, the nanofiber quantum effect and unique physical and chemical properties offer versatile applications in energy storage and production, healthcare, and the environment.[51,80] A wide variety of physical and chemical synthesis techniques such as air-jet spinning, template synthesis, electrospinning, hydrothermal, sol–gel, and electrochemical deposition are used to produce nanofibers.[51,58] Among these, the electrospinning techniques take the lead role, especially in energy storage applications, due to their several advantages, including easily

expanding to the industrial scale from the lab scale.[51] Also, the electrode properties can be further tuned or improved by post-treatment of the spun fibers, like annealing or further deposition of the active electrode.[51,80]

Transition metal oxides in supercapacitors

Transition metal oxides (TMOs) are one of the most studied and considered the best electrode materials for SC applications, especially in pseudo (redox) capacitors.[70,81,82] The availability of different oxidation states for redox reactions helps to achieve very large specific capacitance in TMOs. Ruthenium oxide (RuO$_2$) was one of the first studied pseudocapacitive materials, and shows a theoretical specific capacitance of 700–2000 F g^{-1} with a large potential window of 1.4 V.[83,84] It also shows a very high electrical conductivity on the order of 10^5 S cm^{-1} (nearly metallic) and excellent chemical stability. However, the high crystallinity of RuO$_2$ hinders achieving its theoretical specific capacitance in practical applications.[85] Some recent studies show that different nanostructures and phase-controlled synthesis of RuO$_2$ will help to improve the specific capacitance. For example, a mesoporous rutile structured RuO$_2$ nanotube prepared by a template-assisted method shows a specific capacitance of 1300 F g^{-1}.[86] Even though RuO$_2$ has excellent electrochemical properties, the high cost and low availability

of the material are a major bottleneck in the extensive use of this oxide in SC applications.[42]

Likewise, manganese oxide (MnO_2) is another versatile TMO used extensively in SC and battery applications. Compared to RuO_2, MnO_2 is cheap and widely available, with excellent electrochemical properties. The high specific capacitance (1350 F g^{-1}) with a wide potential window of 0.9 to 1.0 V and the environmental friendliness of MnO_2 make it a perfect choice as an electrode material for supercapacitor applications.[87] The large variety of crystal structures varying from α to β, γ, δ and λ gives peculiar properties like a high surface two-dimensional tunnelling structure, as well as a layered structure, which helps to improve electron transfer and ion intercalation properties in MnO_2.[88] Nevertheless, the poor electrical conductivity (10^{-5} to 10^{-6} S cm^{-1}), low ionic diffusion capability and structural instability are some of the significant drawbacks of MnO_2.[89] Some recent studies show that the nanocomposite approach with carbon compounds (such as graphene, carbon nanotube (CNT), etc.) shows remarkable improvement in the electrochemical properties and stability of the MnO_2-based electrode material.[88] Fig. 3(b) shows the year-wise publications on MnO_2/carbon composite electrodes, and Fig. 3(c) represents different carbon nanomaterials used for composite preparation with MnO_2 electrodes.

Some of the other main TMOs used in the SC industry are iron oxide (Fe_3O_4), which has a better conductivity (10^2–10^3 S cm^{-1}) and natural abundance.[90] Other materials, including cobalt oxide (Co_3O_4), nickel oxide (NiO), copper oxide (CuO), vanadium pentoxide (V_2O_5), titanium dioxide (TiO_2), etc., are also used in SC fabrication. The specific capacitance of different transition metal oxides is depicted in Fig. 3(d) and the main TMOs used for electrospun SCs reviewed in this article are depicted in Fig. 4. Furthermore, the poor cyclability, tendency to form agglomerates in nanoparticles, larger 'dead volume' of the electrode and low electrical conductivity hinder the TMOs from achieving high theoretical specific capacitance.[85,89,91,92]

Electrospun transition metal oxide SCs

Manganese oxide (MnO_x)-based electrospun fiber SCs

Enhancing the electrochemical properties of carbon fiber electrodes by new methodologies and correlating the influence of different dopants and processing parameters on the microstructure during the electrospinning process is a key concern in developing high-performing nanofiber electrodes.[93] Achieving a high mass loading of pseudocapacitive material during electrospinning is a key challenge since it has a huge impact on achieving high gravimetric capacitance.[94] By using 40 wt% manganese acetylacetonate (MnACAC) as the precursor solution for electrospinning to form MnO-doped carbon fibers, in 2018, Liu et al.[59] demonstrated an all fiber-based flexible SC using MnO-doped carbon nanofibers (CNFs) as the electrode and polyacrylonitrile (PAN) as the separator.[59] In order to form MnO-doped carbon fiber, the collected fibers undergo a pre-carbonisation process at 290 °C in air, followed by complete carbonisation at 850 °C in a nitrogen atmosphere for two hours.[59] After the complete carbonisation process, the free-standing flexible fiber mat was cut and used as the electrode for SC fabrication. The photographs and microstructure of the

Fig. 4 Periodic table highlighting the transition metals used for the fabrication of electrospun TMOs in SCs.

Fig. 5 (a) Flexible free standing composite film of PAN-20 wt% MnACAC after carbonisation. (b and c) FE-SEM image of pure PAN fibers (colorized to distinguish orientation) and PAN with 40 Mn@CNF, respectively. (d) Mean diameter of different spun fibers. (e) Variation of specific capacitance with scan rate. (f) Specific capacitances of the all-fiber supercapacitors with different MnACAC concentrations at 2.5 mV s^{-1}. Reproduced from ref. 59 with permission from Elsevier, copyright 2018.

developed fibers are shown in Fig. 5(a)–(d), and the capacitance performance is given in Fig. 5(e) and (f).[59]

The SC with 5 Mn@CNF shows a specific capacitance of 182 F g^{-1}, which is almost double the value compared to the pure PAN-CNF electrode.[59] 1D hollow nanotube-based electrodes having more electroactive sites on both sides of the tube and low ion transportation length can enhance the supercapacitor performances to a further extent by effectively utilizing the surface area.[95] A hollow MnO$_2$ fiber-based electrode was prepared in a two-step process. Initially, CNFs, which act as a guide to the growing MnO$_2$ nanofibers, were prepared via the electrospinning technique using PAN, as discussed earlier, at a carbonisation temperature of 1000 °C in a nitrogen atmosphere for five hours. Finally, the developed CNFs were mixed with KMnO$_4$ solution and undergo a hydrothermal reaction at 140 °C in an autoclave to get nanofibers.[95] The SC's electrochemical performance and galvanostatic charging–discharging analysis (GCD) show a high specific capacity of 291 F g^{-1} at a current density of 1 A g^{-1} and capacitance retention above 90% after 5000 charging–discharging cycles.[95] Schematic representations of hollow nanotube preparation via electrospinning and their microstructures are given in Fig. 6.

Likewise, a low-cost method for fabricating MnO$_2$-decorated electrospun fibers for flexible SC applications was developed by mixing 8 wt% poly(vinylpyrrolidone) (PVP) and Mn(CH$_3$COO)$_2$·4H$_2$O in alcohol–deionized water solvent mixture, followed by electrospinning at a high voltage followed by calcining at 480 °C for five hours.[96] The fabricated supercapacitor has an excellent specific capacitance of 645 F g^{-1} and good capacitance

retention of 95% of its initial value even after 2000 consecutive cycles (Fig. 7(a)–(c)).[96] The better electrochemical performance suggests its potential application in flexible electronics, sensors and other microelectronics.[96] A nanocomposite electrode consisting of MnO$_2$-decorated porous carbon fibers and graphene was prepared via electrospinning followed by thermal annealing using a solution containing a mixture of manganese chloride (MnCl$_2$) dispersed in polymethyl methacrylate (PMMA) and PAN in DMF.[97] Here, the presence of graphene in the electrospinning process helps the uniform distribution of MnO$_2$ particles on the carbon fibers without any agglomeration and helps to improve the conductivity.[97] The electrode with a concentration of 5 wt% graphene gives a better specific capacitance (210 F g^{-1}), good rate capability, and high energy density (24–19 W h kg^{-1}) in an electrolyte of 6 M KOH aqueous solution (Fig. 7(d)–(f)).[97]

Integrating different preparation methods like chemical bath deposition along with electrospinning has shown fascinating results in developing highly efficient fiber electrodes.[98] In a typical process, a fiber electrode was fabricated by growing MnO$_2$ nanosheets on multichannel CNFs doped with amorphous cobalt oxide (CoMCNFs@MnO$_2$) (Fig. 8(a)–(i)).[98] PAN and cobalt acetylacetonate (Coacac)$_3$ were mixed in DMF solvent as a spinning precursor, and the electrospinning process was carried out at 16 kV. Finally, the MnO$_2$ nanosheets were grown in situ on the nitric acid-treated spun fibers from the KMnO$_4$ solution. The advantage of these dual TMO-containing fibers is that they can be used directly without any additional conductive binder. The flexible SC made up of these fibers shows an exceptional electrochemical performance with a
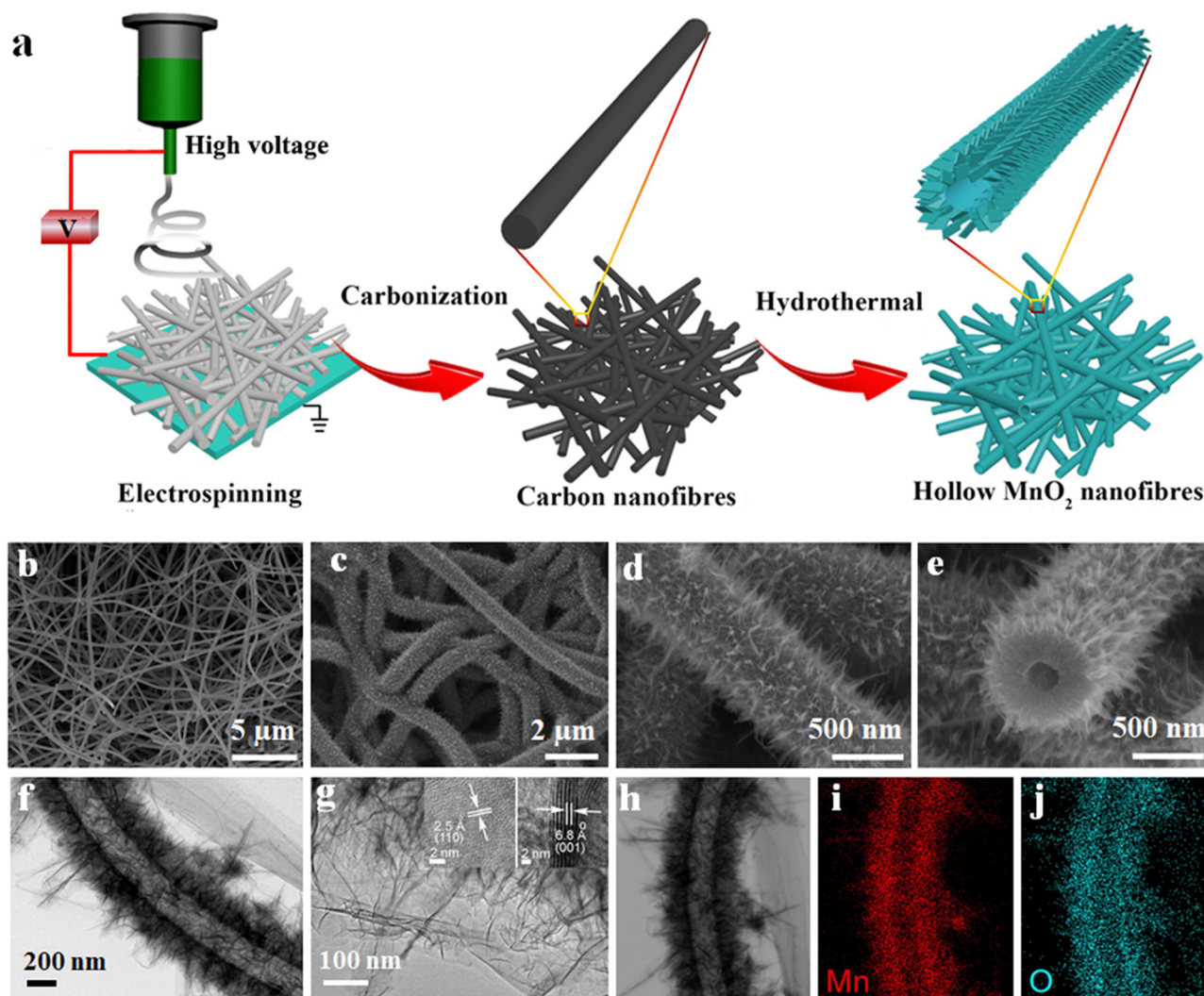
Fig. 6   (a) Schematic of the hollow fiber preparation process. (b)–(e) FE-SEM micrographs of hollow nano fiber. (f and g) TEM micro structure (inset of (g) shows HRTEM images) and (h)–(j) EDS mapping of the MnO$_2$ hollow fiber. Reproduced from ref. 95 with permission from Elsevier, copyright 2018.

specific capacitance of 265 F g^{-1} and a capacitance retention of 98.7% over 10 000 cycles (Fig. 8(j) and (k)).[98]

Similarly, a core–shell-based carbon/MnO$_2$ composite electrode was prepared by the electrospinning technique using the PAN solution in DMF as the core solution, and the PAN/metal source solution as the shell solution to ensure maximum loading of metal oxide particles on the fiber's surface.[99] Here also, the spun fiber mat further undergoes a calcination process at different temperatures to form the electrode. Finally, CO$_2$ gas flowed into the chamber to increase the surface area of the fiber electrode through the interaction of carbon with CO$_2$ gas.[99] The fabricated C–MnO$_x$ composite nanofibers showed better electrochemical performance (specific capacitance of 213.7 F^{-1}, energy density of 30 mW h g^{-1} and capacitive retention of ~97% after 1000 cycles).[99]

Ruthenium oxide (RuO$_2$)-based electrospun fibers

The composite electrode consisting of RuO$_2$ and carbon materials shows enhanced performance due to the synergetic effect of both pseudo and double-layer capacitance. The CNF/RuO$_2$ composite electrode prepared by electrospinning an immiscible polymer blend solution containing PMMA and PAN in the DMF solvent shows increased surface area and porosity.[100] The main advantage of this composition is that due to the low surface tension, the PAN polymer forms a continuous phase compared to the discontinuous phase of PMMA owing to its high surface tension. Hence, upon heat treatment, PAN will convert into CNFs whereas the PMMA will be completely burnt, leaving porosity in the fiber.[100] The precursor solution for this immiscible blend was prepared by mixing ruthenium(III) acetylacetonate with PAN/PMMA in DMF and subjected to electrospinning at an applied voltage of 20 kV.[100] Finally, the spun fibers were stabilized at 280 °C for 1 h in air, then calcined at 700 °C in a steam and nitrogen carrier gas mixture.[100] The microstructures of the spun fibers with different PMMA loadings and variation in specific capacitance are given in Fig. 9(a)–(d).
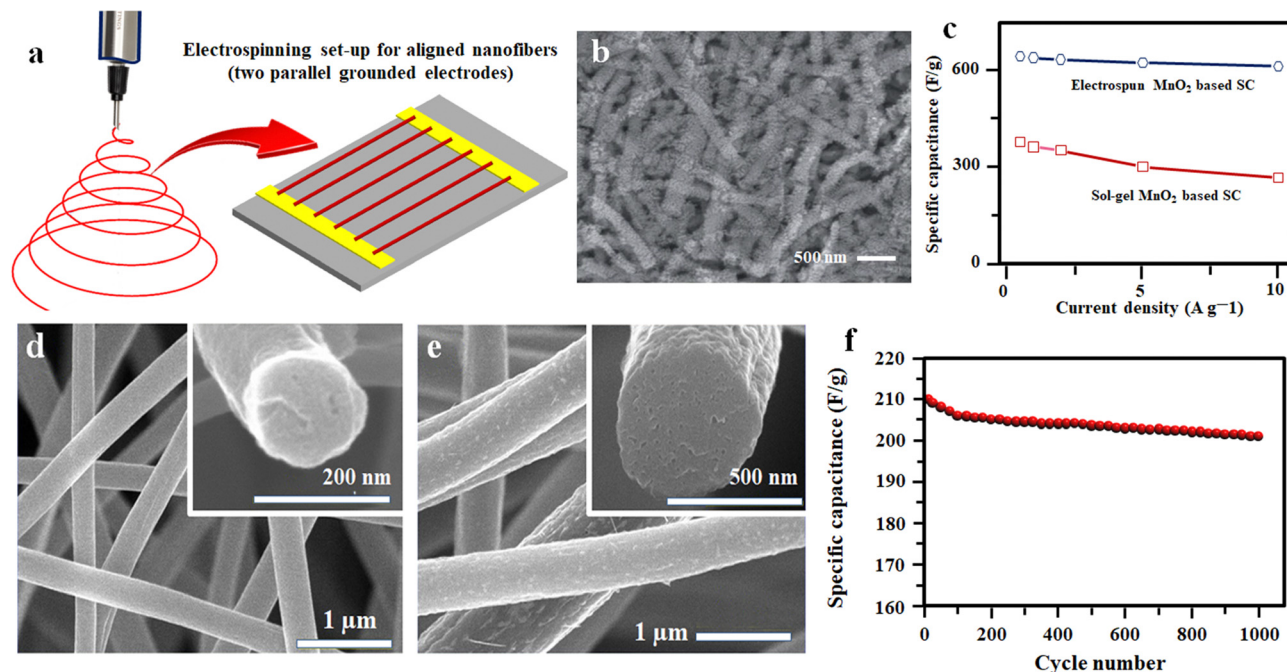
Fig. 7 (a) Schematics of aligned nanofiber preparation. (b) FE-SEM micrographs of MnO$_2$ nanoparticles incorporated after acidation. (c) Comparison of specific capacitance for the electrospun and sol–gel derived MnO$_2$ based SCs. Reproduced from ref. 96 with permission from Royal Society of Chemistry, copyright 2013. (d and e) FE-SEM micrographs of MnO$_2$ on hierarchical porous carbon nano fibers (HPCNFs) with 0 and 5 wt% graphene and (f) cyclic performance of MnO$_2$/HPCNF/G5. Reproduced from ref. 97 with permission from Elsevier, copyright 2016.

The electrochemical performance of the fabricated SC using the spun fiber electrode was analysed, and the results show better energy and power density. The variation of the specific capacitance of diverse ACNF Fiber electrodes with varying current densities is shown in Fig. 9(e). The influence of PMMA addition on creating porosity, surface area and, thereby, electrochemical performance was also correlated, and the results are shown in Fig. 9(f).[100] Likewise, the RuO$_2$ containing CNF with a hollow core structure was prepared by a one-step electrospinning technique using the same immiscible blend of PAN and PMMA.[101] Here, the authors systematically analysed the energy storage efficiency of the developed activated carbon nanofiber (ACNF) containing amorphous RuO$_2$ with different hollow core structures.[101]

Recently, in another approach, the RuO$_2$ nanorods were grown directly by a precipitation method on CNF fibers prepared by the electrospinning technique.[102] Here, at first, Ru(OH)$_3$ was precipitated from RuCl$_3 \cdot x$H$_2$O aqueous solution by carefully adding NaOH solution.[102] The formed Ru(OH)$_3$ was redispersed into ethanol and then drop cast on the CNF fibers. Finally, the samples were heated at 300 °C in an air atmosphere.[102] The microstructure of the developed fibers is shown in Fig. 10(a)–(h).

The specific capacitance of RuO$_2$–CNF and neat CNF represented in Fig. 10(i) shows that RuO$_2$ addition increases the specific capacitance compared to neat CNF. It was also evident from the figure that the amount and annealing temperature of RuO$_2$ influences the total capacitance of the device.[102] A Ragone plot of all the fabricated devices is given in Fig. 10(j) to compare the device performance.[102]

Iron oxide (Fe$_2$O$_3$)-based electrospun fibers

Compared to all other TMOs, Fe$_2$O$_3$ is getting more attention in the SC industry because of its low cost, large availability, and more importantly, its environmental friendliness.[103] Among the different polymorphs, α-Fe$_2$O$_3$ is more suitable for electrochemical applications, including supercapacitors and batteries.[104–107] The performance of the Fe$_2$O$_3$-based electrode varies significantly with its morphology and nanostructure. Similarly, the spinning solution has a critical role in designing the nanoparticle morphology during electrospinning. In this regard, the fabrication of dual morphology of electrospun Fe$_2$O$_3$ electrodes using the same iron oxide precursor in two different polymers was reported.[103] Here, ferric acetylacetonate (Fe(acac)$_3$) was used to prepare the composite electrode as the iron oxide precursor. To synthesise porous Fe$_2$O$_3$ fibers (PFs), the Fe(acac)$_3$ was added into an electrospinning solution containing polyvinyl pyrrolidone (PVP) dissolved in an ethanol and acetic acid mixture.[103] On the other hand, Fe$_2$O$_3$ nanograins (NGs) were prepared by mixing Fe(acac)$_3$ in polyvinyl acetate (PVAc), N,N-dimethyl acetamide (DMAc) and glacial acetic acid mixture.[103]

Interestingly, the change in the polymer matrix resulted in two different morphologies of the Fe$_2$O$_3$ electrode. As represented in schematics (Fig. 11(a)), in the case of PVP, it forms a strong interaction with the metal oxide and is retained between the Fe$_2$O$_3$ particles even after the polymer is burnt out, and the
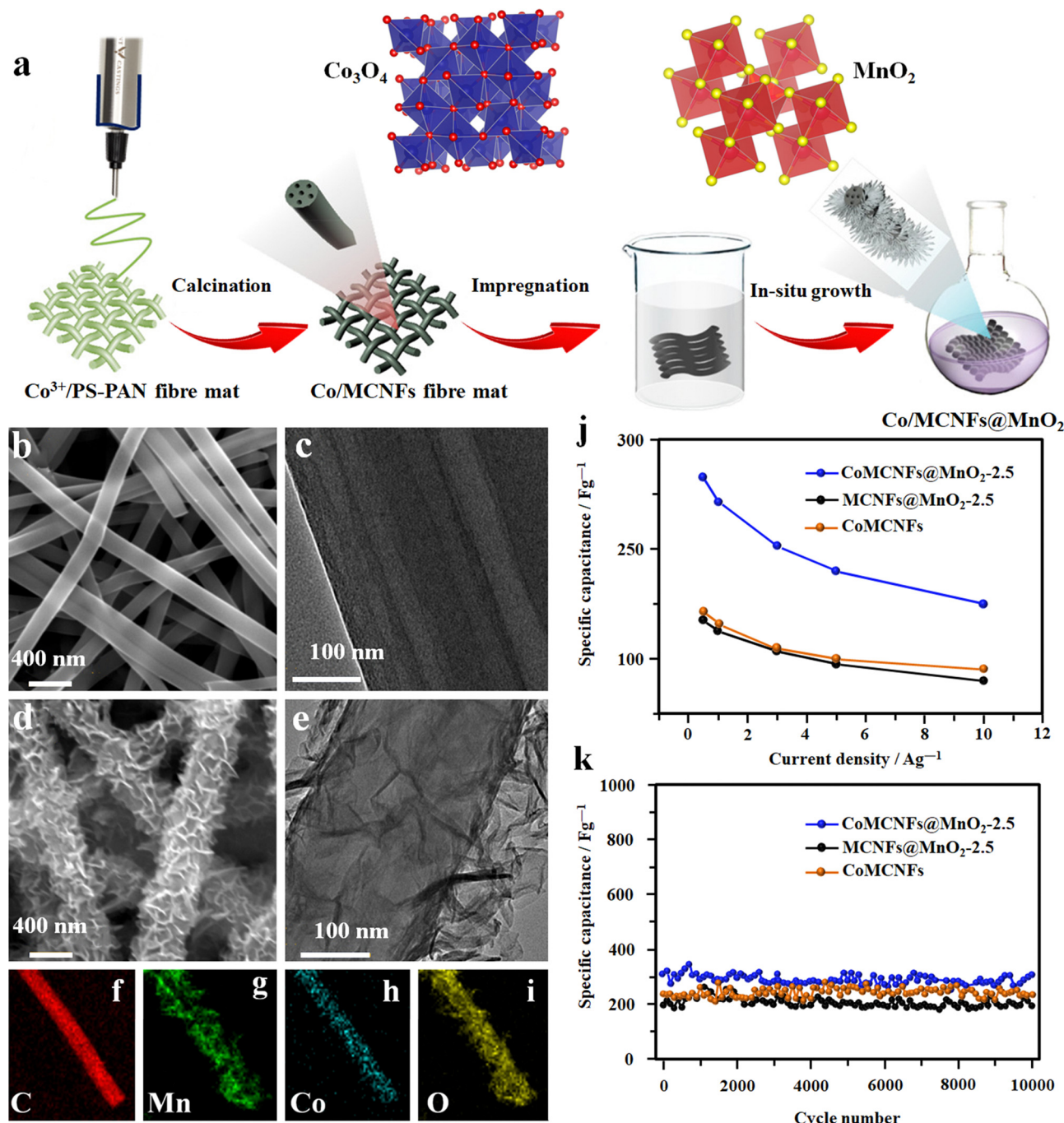
Fig. 8 (a) Schematics of the electrode fabrication of MnO_2 nanosheets on the multichannel carbon nanofibers containing amorphous cobalt oxide (CoMCNFs@MnO_2). FE-SEM and TEM microstructure of: (b) and (c) the CoMCNF electrode, and (d) and (e) CoMCNF@MnO_2-2.5 electrodes respectively. (f)–(i) Scanning tunneling electron microscopy (S-TEM) micrographs of the CoMCNFs@MnO_2-2.5 electrode. (j) Specific capacitance. (k) Cyclic performance of the fiber electrode. Reproduced from ref. 98 with permission from American Chemical Society, copyright 2019.

interaction is responsible for fiber formation.[103] While in the case of PVAc polymer, the weak/reduced interaction with the Fe_2O_3 particles results in phase separation during the calcination to form micrograins (Fig. 11(b)–(e)).[103] The capacitance performance of both PF and NG-based SCs was studied in 1 M lithium hydroxide (LiOH) electrolyte, and the results indicated that the PF-based device shows better performance owing to its porous nature, high aspect ratio and better surface area (Fig. 11(f)).[103] The cycling performance of both devices shows good capacitance retention after 3000 charging–discharging cycles (Fig. 11(g)).[103]

Enhancing the electrochemical performance of fiber electrodes *via* composite preparation shows remarkable properties. The functionalization of Fe_3O_4-coated electrospun
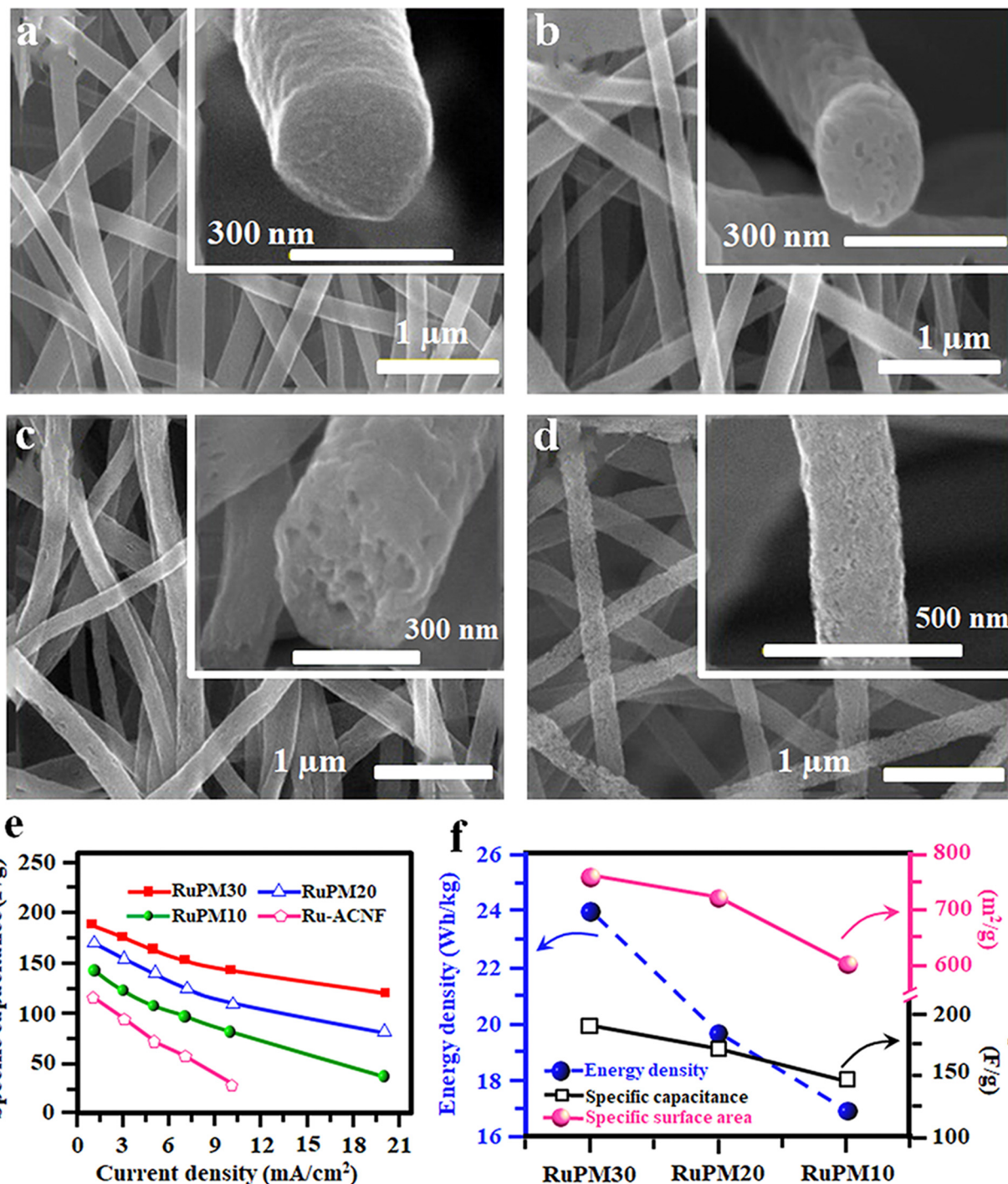
Fig. 9 (a)–(d) FE-SEM micrographs of the Ru-ACNF webs obtained using different concentrations of PMMA after activation. (e) Variation of specific capacitance at different current densities and (f) variation of surface area, specific capacitance and energy density of SC electrodes with PMMA concentration. Reproduced from ref. 100 with permission from Elsevier, copyright 2016.

carbon nanofibers (Fe_3O_4@CNF) by electrodepositing MnO_2 is a different approach for making a composite electrode.[108] The schematic illustration of the same is represented in Fig. 12(a). The microscopic images of the spun fiber are shown in Fig. 12(b) and (c). The developed fiber shows better flexibility than pure CNF, because the doped Fe_3O_4 particles help scatter the stress concentration during

mechanical bending (Fig. 12(d)).[108] The MnO_2 was coated by the electrospray technique using $KMnO_4$ solution, showing enhancement in the electrochemical performance with a high specific capacitance of 360 F g^{-1} and improved retention capacity.[108]

Likewise, a composite nanotube electrode containing vanadium pentoxide (V_2O_5) and α-Fe_2O_3 was fabricated through a

Fig. 10   (a)−(d) FE-SEM images of pure and RuO$_2$-doped CNF. (e)−(h) TEM and EDS analysis of RuO$_2$−CNF. (i) Specific capacitance with different current densities and (j) Ragone plot of RuO$_2$−CNF flexible SC. Reproduced from ref. 102 with permission from American Chemical Society, copyright 2020.

Fig. 11 (a) Schematic showing the interactions of metal oxides with different polymers (PVAc and PVP). (b)–(e) FE-SEM micrographs of as spun and calcined Fe(acac)$_3$–PVP and Fe(acac)$_3$–PVA electrospun fibers, respectively. (f) Discharge curves of PF at various current densities. (g) Comparison of the cycling performance of both PF and NG electrodes. Reproduced from ref. 103 with permission from Royal Society of Chemistry, copyright 2013.

one-step electrospinning process at ambient temperature and relatively low humidity of 20% by dissolving Fe(NO$_3$)$_3$·9H$_2$O and PVP in an equal mixture of DMF and isopropyl alcohol solvents.[109] The precursor vanadyl acetylacetonate (VO(acac)$_2$) was mixed with the above solution prior to electrospinning.[109] Finally, the spun fiber matt was calcined at 450 °C for 3 h in an air atmosphere. The spun fiber shows good ferromagnetic

properties, and its magnetization capacity increases with V$_2$O$_5$, apart from its better electrochemical activity.[109] The electrochemical performance of the developed nanofiber was characterized by CV and GCD analysis. The microstructure and electrochemical results are given in Fig. 13(a)–(c).[109] In the composite approach, the fiber electrode shows enhancement in properties with dopant addition.

Fig. 12 (a) Schematics of flexible Fe_3O_4@CNFMn electrode preparation. (b and c) FE-SEM micrographs of the Fe_3O_4@CNF and Fe_3O_4@CNFMn fiber electrode respectively. (d) Photographs and mechanism of the enhanced flexibility of the Fe_3O_4@CNFMn electrode. Reproduced from ref. 108 with permission from Nature, copyright 2017.
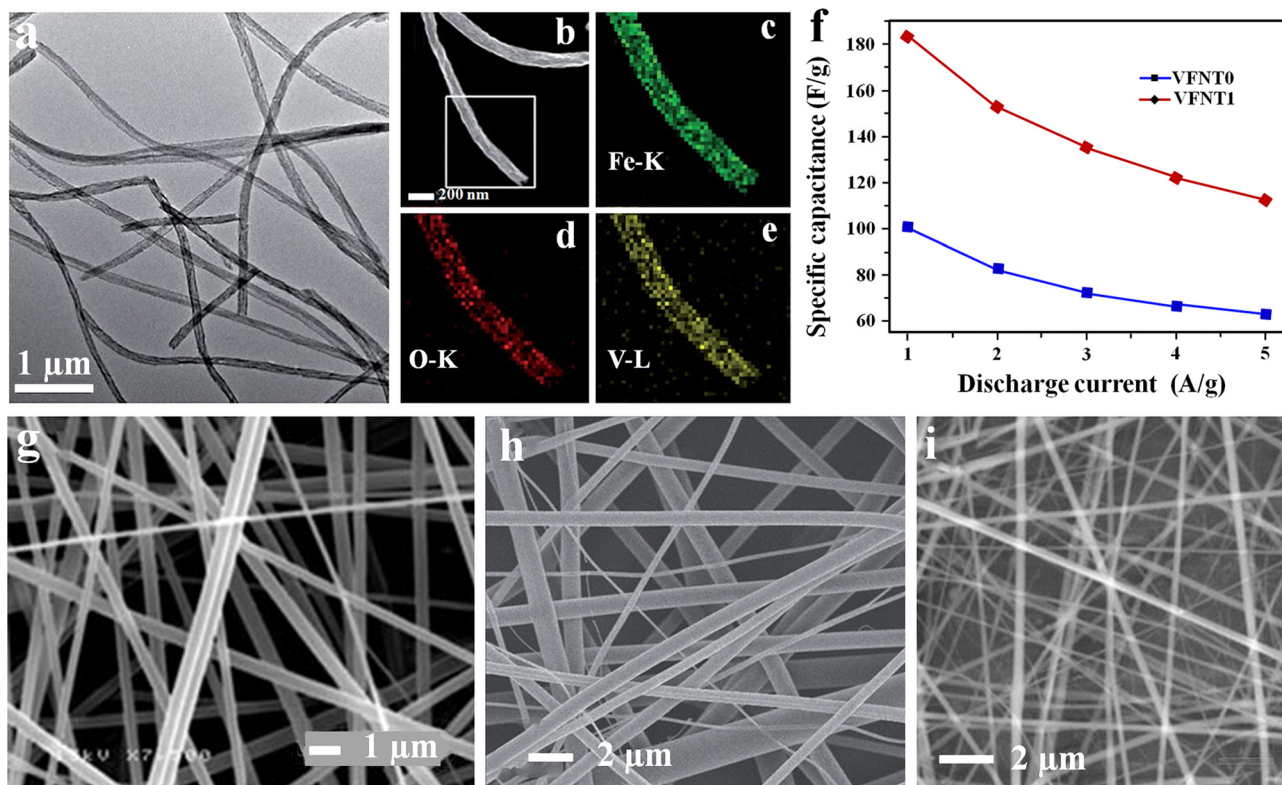
Fig. 13 (a) TEM microstructure V_2O_5/1 wt% Fe_2O_3. (b)–(e) HAADF–STEM pattern and EDX mapping. (f) Variation of the specific capacitance of V_2O_5 (VFNT0) and V_2O_5/1 wt% Fe_2O_3 (VFNT1) at different current densities. Reproduced from ref. 109 with permission from Royal Society of Chemistry, copyright 2014. FE–SEM micrographs of electrospun fibers of: (g) V_2O_5, reproduced from ref. 111 with permission from Royal Society of Chemistry, copyright 2010; (h) as-spun V_2O_5 nanofibers, reproduced from ref. 112 with permission from Wiley, copyright 2012 and (i) graphene oxide/V_2O_5 nanofiber, reproduced from ref. 113 with permission from Elsevier, copyright 2014 respectively.

Vanadium pentoxide (V_2O_5)-based electrospun fibers

Vanadium oxide and its nanocomposites with different morphologies such as nanotubes, nanorods, *etc.* have been used extensively in energy storage applications, including lithium ion batteries due to their variable oxidation states and layered structure.[110,111] The use of electrospun V_2O_5 fibers as an electrode for supercapacitors for the first time was reported in 2010. Herein, electrospinning was carried out using PVP and vanadyl acetylacetonate (VO(acac)$_3$) dissolved in ethanol, and acetic acid as the precursor solution at a positive potential of 10 kV, and the spun fiber was calcined at 300–500 °C. The electrochemical performance of the fiber electrode was characterized using a 3-electrode setup in both aqueous (2 M KCl, 2 M KOH, 1 M H_2SO_4) and organic (1 M $LiClO_4$ in propylene carbonate) electrolytes at room temperature and a maximum specific capacitance of 190 F g^{-1} was obtained for the KCl electrolyte. As it is a well-known factor that both energy and power density depends on the operating potential, the fiber electrode in organic electrolyte shows high energy and power density of 78 W h kg^{-1} and 1.8 kW kg^{-1}, respectively, compared to 5 W h kg^{-1} and 1.7 kW kg^{-1} in the KCl electrolyte.[111] Likewise, a high energy density hybrid SC was constructed using an electrospun V_2O_5 in a carbon nanotube network.[112] The fabricated SC delivered maximum energy and power densities of 18 W h kg^{-1} and 315 W kg^{-1}, respectively.[112] Similarly,

the SC developed using the graphene oxide/V_2O_5 (GVO) nanofiber electrode shows better specific capacitance and electrochemical properties.[113] The microstructures of different V_2O_5-based spun fibers are given in Fig. 13(d)–(f).[111–113]

Nickel oxide (NiO)-based electrospun fibers

NiO having better specific capacitance (2573 F g^{-1}), low cost, nontoxicity and environmental friendliness is a suitable candidate for energy storage applications, including SCs and batteries.[26,114,115] An asymmetric SC using NiO as the cathode by a sol–gel assisted electrospinning process and activated carbon as the anode material in KOH electrolyte showed remarkably high specific capacitance of 141 F g^{-1} with an energy and power density of 43.75 W h kg^{-1} and 7.5 kW kg^{-1}, respectively.[116] The synergic contribution of electrical double layer capacitance from the carbon electrode and pseudocapacitance from NiO were responsible for this enhanced performance of the asymmetric SC (ASC). The ASC also shows better capacitance retention of 88% and improved coulombic efficiency of 93% over 5000 charge–discharge cycles.[116] Similarly, the SC fabricated using NiO nanowires prepared by electrospinning a polymeric solution containing nickel acetate tetrahydrate and polyvinyl alcohol shows a better specific capacitance of 670 F g^{-1}.[117] Introducing porosity on NiO nanofibers by direct electrospinning on a Ni-foam current collector followed
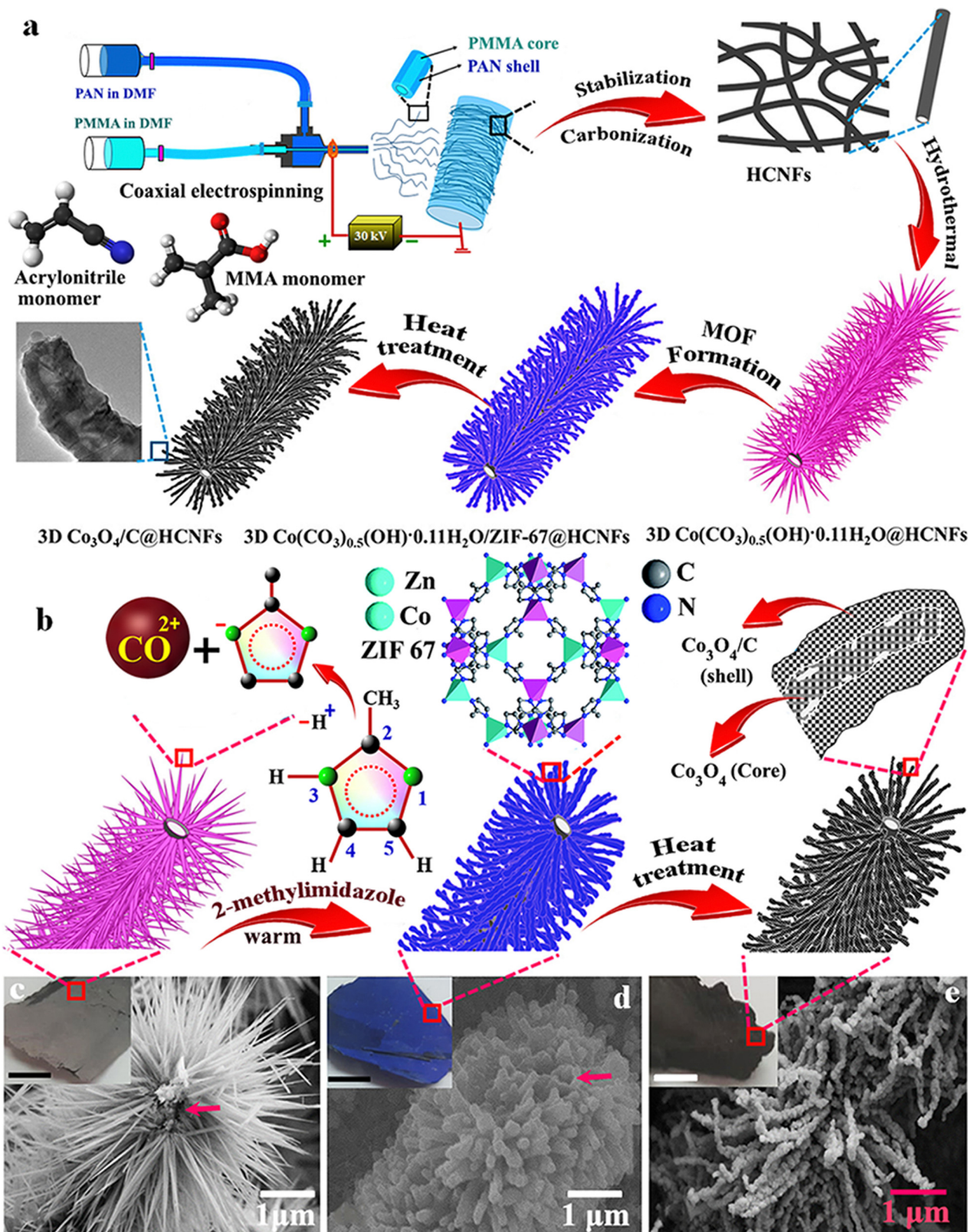
Fig. 14 (a and b) Schematic and mechanism of the fabrication of 3D Co_3O_4/C@HCNF nanocomposites. FE-SEM image of (c) $Co(CO_3)_{0.5}OH\cdot0.11H_2O$@HCNFs, (d) $Co(CO_3)_{0.5}OH\cdot0.11H_2O$/ZIF-67@HCNFs and (e) Co_3O_4/C@HCNFs. Reproduced from ref. 121 with permission from American Chemical Society, copyright 2020.

by heat treatment can result in an interconnected network structure on the foam, which will help improve the ion transport mechanism and electrochemical activity.[118] The electrochemical analysis of the developed fiber shows reasonably high specific capacitance (737 F g^{-1} at 2 A g^{-1}), excellent rate capability with high capacitance retention and good cycling stability up to 8000 cycles.[118] Equally, the N-doped CNF using polyacrylonitrile and acetyl acetone as the precursor with uniformly dispersed NiO nanoparticles displays a specific capacitance (850 F g^{-1}), long life cycle and enhanced rate capability.[119]

Cobalt oxide (Co$_3$O$_4$)-based electrospun fibers

Like other TMOs, Co$_3$O$_4$ also has a very high theoretical specific capacitance of 3560 F g^{-1}.[120] In recent times, plenty of research has been going on to use Co$_3$O$_4$ as a suitable electrode material for SC applications by changing its morphology and nanostructure. In this regard, electrospun fiber-based electrodes are getting more attention. Similarly, a metal–organic framework (MOF)-based electrode with very high porosity and surface area has also attracted considerable interest in energy storage. Recently, a composite electrode consisting of a hollow carbon nanofiber (HCNF) mat prepared by electrospinning and Co$_3$O$_4$/C nano tentacles grown from a cobalt hydroxide precursor has

shown high porosity and surface area, and enhanced electrochemical performance.[121] The as-prepared hollow 3D Co$_3$O$_4$/C@HCNFs nanocomposite sheet exhibits a specific capacity of 1623 F g^{-1} at a current density of 1 A g^{-1}.[121] The ASC fabricated using the prepared fiber as the positive electrode and nitrogen-doped graphene hydrogel (NGH) as the negative electrode provides an energy density of 36.6 W h kg^{-1} at a power density of 471 W kg^{-1} with outstanding rate capability.[121] A schematic of nanofiber preparation and the obtained microstructure is shown in Fig. 14. In a similar approach, a ternary nanocomposite was prepared by growing mesoporous cobalt oxide nanohairs (Co$_3$O$_4$ nanohair) and silver nanoparticles (AgNPs) on an electrospun carbon nanofiber (schematics shown in Fig. 15).[122] These highly conductive (AgNPs and CNF) and electroactive constituents (Co$_3$O$_4$ nanohair) lead to high capacitance, long lifetime and high rate capability of the nanocomposite. The optimized electrode fiber exhibits a specific capacitance of 1880 F g^{-1} at a current density of 2 A g^{-1} and the asymmetric supercapacitor assembled with NGH exhibits a high energy and power density of 53.8 W h kg^{-1} and 797.9 W kg^{-1}, respectively.[122]

Similarly, the ASC fabricated using Co$_3$O$_4$ nanowires prepared by an aqueous polymeric solution-based electrospinning process as the anode and commercial activated carbon (AC) as

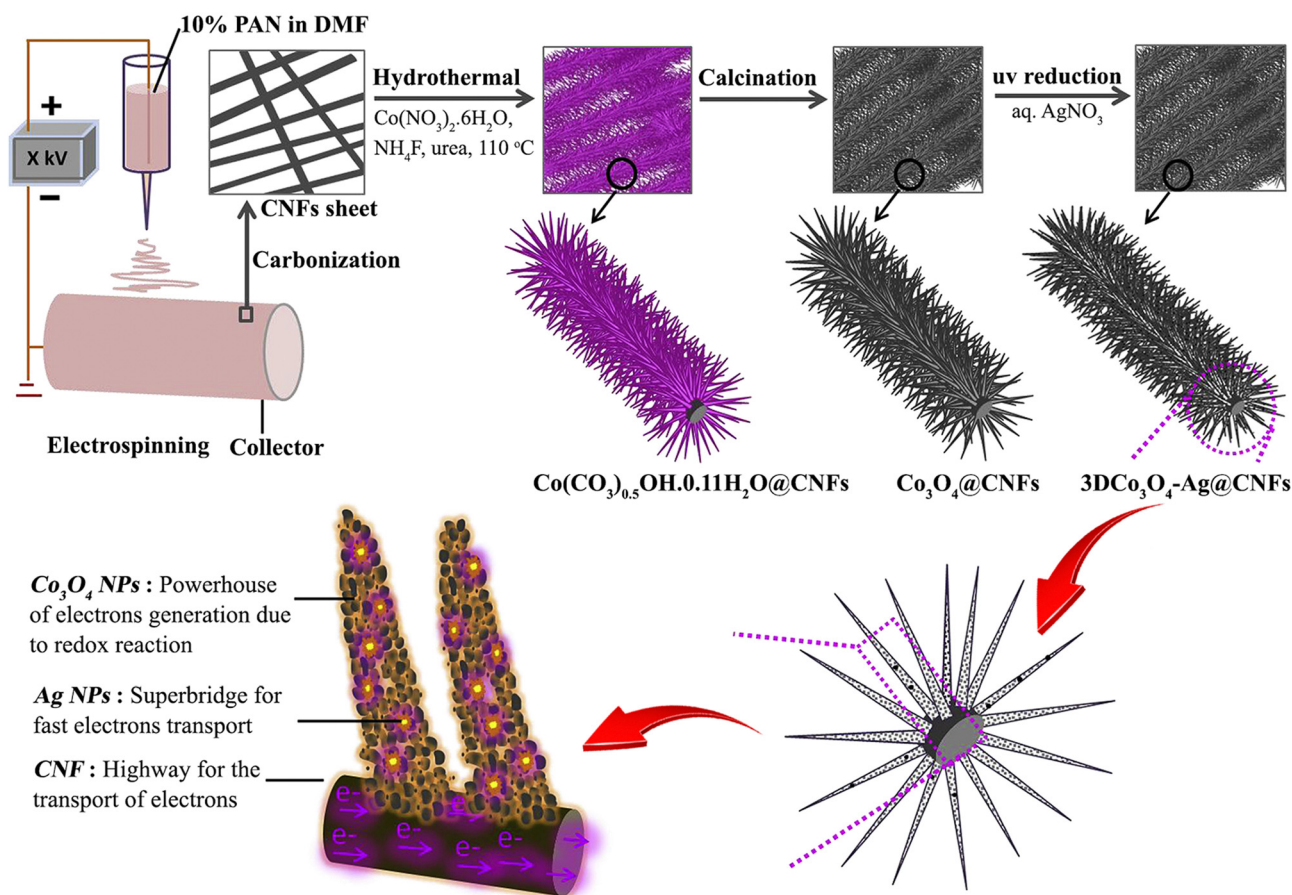Fig. 15 Schematic representation of 3D Co$_3$O$_4$–Ag@CNFs nanocomposite electrode preparation, its microstructure and the role of different materials in SC performance. Reproduced from ref. 122 with permission from Elsevier, copyright 2019.

the cathode shows a specific capacitance of 175 F g^{-1}.[123] The individual Co_3O_4 nanowires show a high specific capacitance of 1110 F g^{-1} in 6 M KOH compared to Co_3O_4 nanofibers prepared by electrospinning in a different approach having a specific capacitance of 407 F g^{-1} at a scan rate of 5 mV s^{-1}.[124] Table 1 summarizes the different spinning conditions used for the TMO-based nanofiber preparation and their electrochemical properties for advanced SC applications.

Bimetal transition metal oxide-based electrospun fibers for supercapacitor applications

Nowadays, apart from the single metallic oxides, bimetallic TMOs are getting more attention due to their high specific capacitance, improved electrical conductivity and better faradaic reactions than their single transition metal oxide counterparts.[125–129] Combining more than one metal oxide will introduce a difference in the Fermi energy levels along with augmenting the affinity between the oxides and also improving the intrinsic electrical conductivity and long-term stability.[130] This will eventually enhance the range of stable potential window. There are a few reports available on fabricating bimetallic TMO nanofibers as high performing supercapacitor electrodes through electrospinning techniques. Recently, to enhance the electrochemical performance of manganese oxide (Mn_2O_3), a bimetallic nanocomposite approach was introduced.[131] Herein, a composite nanofiber electrode of Mn_2O_3 with spinel $ZnMn_2O_4$ (ZMO) was prepared by electrospinning. The resultant nanofiber composites show improved charge transport kinetics and large activation sites. The incorporation of the ZMO phase in Mn_2O_3 resulted in an enhancement in its electrical conductivity and capacitance. The electrochemical studies of the electrospun composite fiber (Mn_2O_3 – 1 wt% ZMO) show a maximum specific capacitance of 360 F g^{-1} at a current density of 0.1 A g^{-1}. A remarkable capacitance retention of about 98% after 3000 cycles was shown by this composite, indicating property enhancement in the Mn_2O_3 electrode through the bimetallic composite approach. Similarly, in another study, a flexible freestanding film of bimetallic $ZnMn_2O_4$ carbon nanofiber (CNF) electrodes was prepared by the electrospinning technique using the acetate salts of zinc and manganese.[130] The flexibility, microstructure and porosity of the spun fiber were tuned by adjusting the ratio of the mixture with the additional use of terephthalic acid (TPA) and sodium dodecyl sulfate. The morphology and microstructure of the various spun fiber composites with mapping of different elements present in the fiber are given in Fig. 16. Electrochemical analysis reveals a wide potential window of 1.6 V in 6 M KOH electrolyte for the composite fiber electrode with very good specific capacitance (1080 F g^{-1} at 1 A g^{-1}) and capacitance retention (92% after 10 000 galvanostatic charge–discharge cycles).

Table 1 List of spinning conditions and electrochemical performance of TMO-based electrospun fiber SCs

Material	Precursor	Spinning conditions[a]		Specific capacitance (F g^{-1})	Energy density (W h kg^{-1})	Ref.
		Voltage (kV)	Feed rate (mL h^{-1})			
MnO doped CNF	PAN/DMF/MnACAC	10	—	182	—	59
MnO_2 hollow fiber	PAN/DMF/MnACAC	12	0.8	291	—	95
MnO_2 nanoparticles	PVP/Mn(CH$_3$COO)$_2$·4H$_2$O	10–15	0.3	645	—	96
MnO_2/HPCNF/G	MnCl$_2$/PMMA and PAN/DMF	—	—	210 (1 mA cm^{-2}) 170 (20 mA cm^{-2})	24–19	97
CoMCNFs@$MnO_{2-2.5}$	PS/PAN/(Coacac)$_3$/DMF	16	—	265 (0.5 A g^{-1})	19.27	98
Carbon/MnO_2 composite	PAN/DMF/PAN/metal source	6 ± 1	—	213.7 (0.5 A g^{-1})	30	99
CNF/RuO_2 composite	(C$_5$H$_7$O$_2$)$_3$Ru/PAN/PMMA/DMF	20	—	116–188 (1 mA cm^{-2})	14–24	100
RuO_2/CNF hollow core	RuO$_2$/PAN/PMMA/DMF	20	—	180	20–14	101
RuO_2 nanorods	Ru(OH)$_3$/PAN/DMF	—	—	188	22–15	102
α-Fe$_2$O$_3$ porous fiber	PFs/PVP/C$_2$H$_6$O/CH$_3$COOH/Fe(acac)$_3$	10	1	256	13	103
α-Fe$_2$O$_3$ nano grains	PVAc/DMAc/CH$_3$COOH/Fe(acac)$_3$	15	—	102	—	103
Fe$_3$O$_4$@CNF/MnO$_2$	KMnO$_4$/PVA/PAN/Fe(acac)$_3$/DMF	15	1	306	13	108
(V$_2$O$_5$) and α-Fe$_2$O$_3$	PVP/DMF–IPA, VO(acac)$_2$	18	—	150	—	109
V$_2$O$_5$ nanofiber	PVP and VO(acac)$_2$/C$_2$H$_6$O/CH$_3$COOH	10	2	190 (2 M KCl) 250 (1 M LiClO$_4$/PC)	5 78	111 111
V$_2$O$_5$ nanofibers with CNT	PVP & VO(acac)$_2$/C$_2$H$_6$O/CH$_3$COOH	10	2	135	18	112
GO/V$_2$O$_5$ (GVO) nanofiber	VO(acac)$_2$, GO/PVP/DMF	24	—	—	—	113
NiO nanofibers	NiAc–PVP sol–gel	20	1	141	43.75	116
NiO nanowires	C$_4$H$_{14}$NiO$_8$/PVA	24	0.5	670	—	117
NiO nanofiber	Ni(CH$_3$COO)$_2$.4H$_2$O/C$_6$H$_8$O$_7$.H$_2$O/PVP/H$_2$O	25	2	737	22.7	118
N-doped porous CNF (NiO/PCNF)	C$_{10}$H$_{14}$NiO$_4$/PAN/DCDA	—	—	850	—	119
Co$_3$O$_4$/C@HCNFs nanocomposite	Co(CO$_3$)$_{0.5}$OH.0.11H$_2$O/PAN/PMMA/DMF	30	0.02	1623	36.6	121
Co$_3$O$_4$ nanowires	CoAc/PVA/H$_2$O	24	0.5	1110	8.4	123
ASC fabricated using Co$_3$O$_4$				$\sim$175	47.6	
Co$_3$O$_4$ nanofibers	(CH$_3$COO)$_2$Co.4H$_2$O/PVP/C$_2$H$_6$O	13.5	0.5	407	—	124
3D Co$_3$O$_4$–Ag@CNFs	—	18	0.6	1880	53.8	122

[a] Tip distance 8–20 cm.

Furthermore, nickel and cobalt-based bimetal oxide supercapacitor electrodes on carbon nanofibers coated with carbon ($NiCo_2O_4$@C/CNFs) were prepared by a technique combining both electrospinning and electrospraying processes.[132] In this process, the electrospinning precursor solution for the carbon nanofibers was prepared by dissolving PAN in DMF, whereas the electrospraying solution of $NiCo_2O_4$ was prepared by dispersing the nanoparticles in DMF solution. Both these solutions were loaded in the spinning unit and a voltage of 15 kV was maintained with feed rates of 4 mm h^{-1} (electrospinning) and 6 mm h^{-1} (electrospray). From the morphological analysis,

$NiCo_2O_4$ clusters were homogeneously allocated and tightly tangled in the CNF network with a size range of 5–10 μm. The prepared fiber electrodes showed a high specific capacitance of 1586 F g^{-1} at 1 A g^{-1} and a good rate performance. Likewise, another nickel–cobalt bimetallic oxide electrospun carbon nanofiber ($Ni_xCo_{0.5-x}$Oxide/ECNF) electrode was prepared as a free-standing supercapacitor electrode without any binder or conductive agents.[125] Among the various composite electrodes prepared, the one with composition $Ni_{0.25}Co_{0.25}$Oxide exhibited the highest specific capacitance of 697.5 F g^{-1} with more than 94% capacitance retention even after 2000
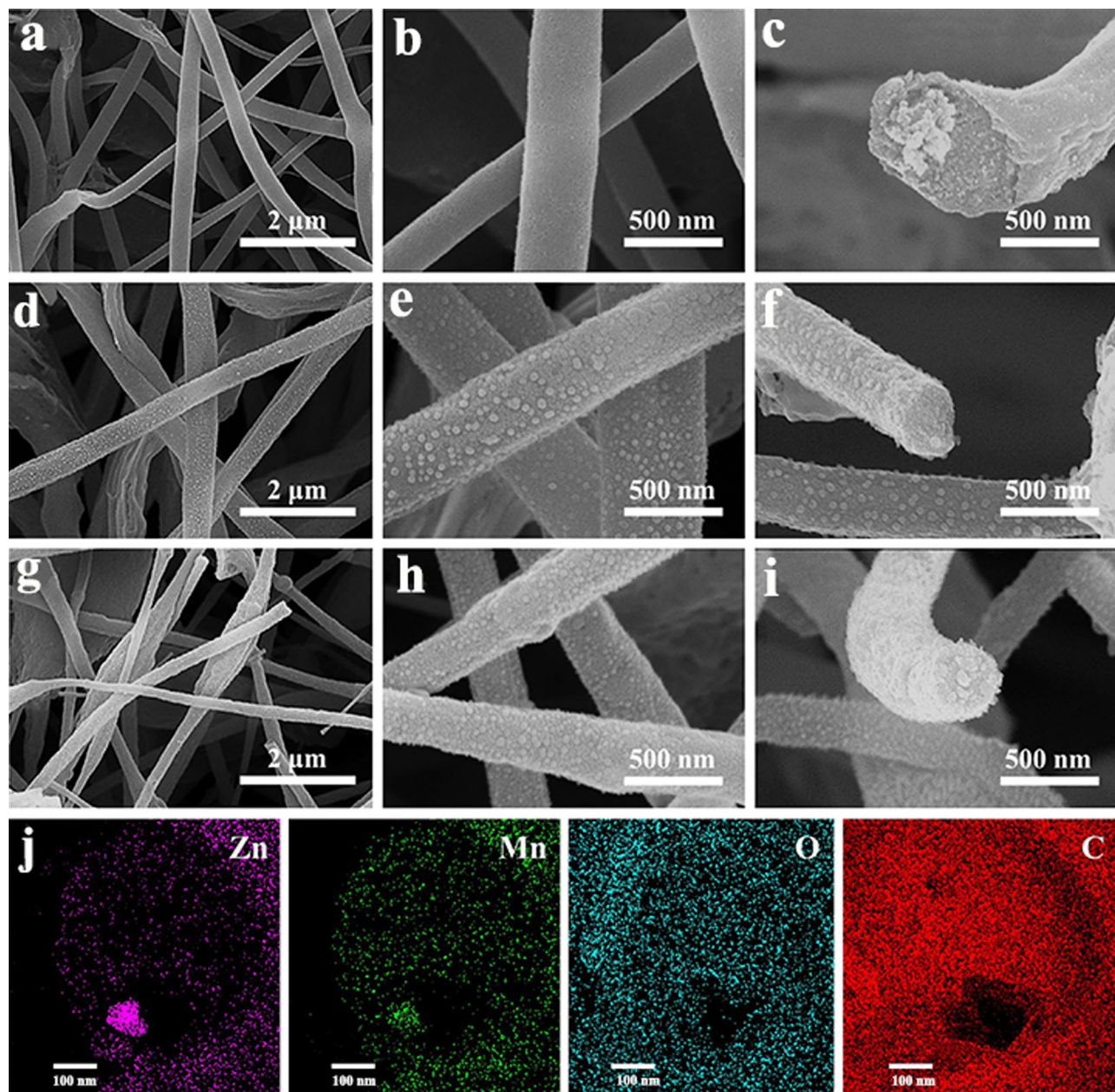
Fig. 16 FE-SEM micrographs of Zn–Mn bimetallic oxides with varying ZnAc/MnAc ratio: (a) and (b) ZMTS1 (ZnAc : MnAc = 1 : 3); (d) and (e) ZMTS2 (ZnAc : MnAc = 2 : 2); (g) and (h) ZMTS3 (ZnAc:MnAc = 3 : 1) at different magnification. (c), (f) and (i) Corresponding cross-sectional images of ZMTS1, ZMTS2 and ZMTS3, respectively. (j) The elemental mapping of different elements such as Zn, Mn, O and C present in the CNFs (ZMTS3). Reproduced from ref. 130 with permission from Wiley, copyright 2022.

charging–discharging cycles at a high current density of 10 A g^{-1}. Moreover, a 1D ZnCo$_2$O$_4$/C composite was recently prepared by the electrospinning technique.[133] Here, the microstructural analysis of the calcined fiber depicts an interesting observation that as the temperature increases, the fibre diameter decreases and this is attributed to the crispation happening in the fiber with higher temperature. The detailed structural analysis indicates that the single nanofiber of ZnCo$_2$O$_4$/C consists of polycrystalline ZnCo$_2$O$_4$ and C nanoparticles. The electrochemical performance of the nanofiber was studied, and it shows a specific capacitance of 327.5 F g^{-1} at a current density of 0.5 A g^{-1}, which is three times higher than that of the powder electrode of ZnCo$_2$O$_4$ (90.6 F g^{-1}) made by the sol–gel technique. Likewise, another bimetallic manganese–iron oxide nanofiber was prepared through the electrospinning technique as a free-standing film for a supercapacitor electrode without any binder or conducting substrate.[134] The prepared electrodes show excellent stability and flexibility during mechanical bending. The electrochemical studies reveal that the SC with the fiber electrode has a very high specific capacitance of 467 F g^{-1} at a current density of 1 A g^{-1} and a greater capacitance retention above 94% after 10 000 charge discharging cycles.

These results indicate that the electrospun fiber electrodes of bimetal transition metal oxides have excellent capacitance, life cycle and stability in electrochemical performance. This improvement is due to the synergetic contribution of different metal oxides on the faradaic charge/discharge process as well as enhanced electrical conductivity. This will definitely accelerate the research on multi transition metal oxide (MTMO)-based fiber electrodes in supercapacitor applications and also contribute to meeting the ever-increasing demand for functional materials in wearable and optoelectronic devices.

Conclusion and future perspectives

SCs are considered as sustainable energy storage devices for different applications like healthcare, robotics, wearables, *etc.* In SCs, the material architecture and properties are essential deciding factors for attaining high performance in energy and power density, life cycle, charging–discharging rate, cost and sustainability. Nanofiber-based TMOs perform better due to their porous structure and high surface area. Nevertheless, the preparation and control of the nanofiber morphology remains challenging. Among the different synthesis techniques, electrospinning has better size and shape control for large-scale nanofiber production. Polymer-assisted electrospinning of TMOs helps to attain uniform distribution of TMOs on the carbon nanofiber, which helps improve the specific capacitance and enhance the conductivity of the fiber electrode. The variation of different spinning parameters like applied voltage, feed rate, temperature, humidity and working distance primarily affect the size and aspect ratio of the fiber formed. The electrospinning technique also allows the preparation of composite electrodes through a single spinning stage, which helps

to manipulate the electrode composition easily in a cost-effective manner. In most cases, the synergic contribution of EDLC and pseudocapacitance from CNFs and TMOs further helps to enhance the SC energy and power density. In short, there are tremendous advantages for electrospun fiber-based TMO electrodes in SC practical applications. Meanwhile, there are some disadvantages like low packing density of the spun fibers, which hinders achieving the maximum specific capacity as well as the volumetric energy density of the material. Different approaches are employed to address these issues, such as alignment of the spun fibers using specially designed collectors (rotatory) during electrospinning, uniaxial pressing of the spun fiber mat, tuning the pore structure and dimension of the fiber electrode and so on. At the same time, bi and multi-metal-based TMOs are increasingly used in SC electrodes to improve the electrical conductivity and specific capacitance. This opens up new avenues and opportunities for researchers and technologists to improve the performance of the fiber electrode and devices by manipulating the spinning conditions, using multi-metal transition metal oxides and nanocomposite approaches.

Author contributions

Abhilash Pullanchiyodan: conceptualization, writing – draft, creating the graphics, investigation, reviewing and editing; Roshny Joy: writing draft and editing; Pranav Sreeram: writing draft, creating the graphics, and editing; Leya Rose Raphael: reviewing and editing; Akhila Das: reviewing and editing; Neethu T. M. Balakrishnan: reviewing and editing; Jou Hyon Ahn: reviewing and editing; Alexandru Vlad: reviewing and editing; Sivaramapanicker Sreejith: supervision, reviewing and editing; Prasanth Raghavan: conceptualization, supervision, writing – draft, creating the graphics, reviewing and editing.

Conflicts of interest

There are no conflicts to declare.

Acknowledgements

Notes and references

1 M. A. A. Mohd Abdah, N. H. N. Azman, S. Kulandaivalu and Y. Sulaiman, *Sci. Rep.*, 2019, **9**, 1–9.
2 Q. Z. Zhang, D. Zhang, Z. C. Miao, X. L. Zhang and S. L. Chou, *Small*, 2018, **14**, 1–15.

3 M. Zheng, X. Xiao, L. Li, P. Gu, X. Dai, H. Tang, Q. Hu, H. Xue and H. Pang, *Sci. China Mater.*, 2018, **61**, 185–209.

4 S. A. Han, J. Lee, J. Lin, S. W. Kim and J. H. Kim, *Nano Energy*, 2019, **57**, 680–691.

5 G. Zhang, X. Xiao, B. Li, P. Gu, H. Xue and H. Pang, *J. Mater. Chem. A*, 2017, **5**, 8155–8186.

6 R. Liang, Y. Du, P. Xiao, J. Cheng, S. Yuan, Y. Chen, J. Yuan and J. Chen, *Nanomaterials*, 2021, **11**(5), 1248, DOI: **10.3390/nano11051248**.

7 P. F. Teh, S. S. Pramana, Y. Sharma, Y. W. Ko and S. Madhavi, *ACS Appl. Mater. Interfaces*, 2013, **5**, 5461–5467.

8 S. K. Vineeth, M. Tebyetekerwa, H. Liu, C. B. Soni, N. Sungjemmenla, X. S. Zhao and V. Kumar, *Mater. Adv.*, 2022, **3**, 6415–6440.

9 D. Ahuja, V. Kalpna and P. K. Varshney, *J. Phys. Conf. Ser.*, 2021, **1913**, 012065, DOI: **10.1088/1742-6596/1913/1/012065**.

10 A. Ray, A. Roy, S. Saha and S. Das, *Science, Technology and Advanced Application of Supercapacitors*, IntechOpen, 2019, pp. 1–15.

11 E. Troschke, M. Oschatz and I. K. Ilic, *Exploration*, 2021, **1**, 20210128.

12 B. E. Conway, *Electrochemical Supercapacitors*, Springer, US, Boston, MA, 1999.

13 M. Winter and R. J. Brodd, *Chem. Rev.*, 2004, **104**, 4245–4269.

14 I. Jeerapan, J. R. Sempionatto, A. Pavinatto, J. M. You and J. Wang, *J. Mater. Chem. A*, 2016, **4**, 18342–18353.

15 Q. Meyer, Y. Zeng and C. Zhao, *Adv. Mater.*, 2019, **31**, 1–25.

16 C. V. V. Muralee Gopi, R. Vinodh, S. Sambasivam, I. M. Obaidat and H. J. Kim, *J. Energy Storage*, 2020, **27**, 101035.

17 Poonam, K. Sharma, A. Arora and S. K. Tripathi, *J. Energy Storage*, 2019, **21**, 801–825.

18 Z. Zhang, C. Zuo, Z. Liu, Y. Yu, Y. Zuo and Y. Song, *J. Power Sources*, 2014, **251**, 470–475.

19 X. Liang, A. Garsuch and L. F. Nazar, *Angew. Chem., Int. Ed.*, 2015, **54**, 3907–3911.

20 M. K. Aslam, Y. Niu and M. Xu, *Adv. Energy Mater.*, 2021, **11**, 2000681, DOI: **10.1002/aenm.202000681**.

21 J. S. Lee, S. T. Kim, R. Cao, N. S. Choi, M. Liu, K. T. Lee and J. Cho, *Adv. Energy Mater.*, 2011, **1**, 34–50.

22 B. E. Conway, *Electrochemical Supercapacitors*, Kluwer Academic/Plenum Publishers, 2002.

23 Sungjemmenla, C. B. Soni, S. K. Vineeth and V. Kumar, *Adv. Energy Sustain. Res.*, 2022, **3**, 2100157.

24 S. Zhang and N. Pan, *Adv. Energy Mater.*, 2015, **5**, 1–19.

25 A. Pullanchiyodan, L. Manjakkal, M. Ntagios and R. Dahiya, *ACS Appl. Mater. Interfaces*, 2021, **13**, 47581–47592.

26 A. Pullanchiyodan, L. Manjakkal, S. Dervin, D. Shakthivel and R. Dahiya, *Adv. Mater. Technol.*, 2020, **5**, 1901107, DOI: **10.1002/admt.201901107**.

27 N. Kurra, R. Wang and H. N. Alshareef, *J. Mater. Chem. A*, 2015, **3**, 7368–7374.

28 X. Chen, R. Paul and L. Dai, *Natl. Sci. Rev.*, 2017, **4**, 453–489.

29 S. Zhu, J. Ni and Y. Li, *Nano Res.*, 2020, **13**, 1825–1841.

30 N. Jabeen, A. Hussain, Q. Xia, S. Sun, J. Zhu and H. Xia, *Adv. Mater.*, 2017, **29**, 1–9.

31 K. G. Cho, H. S. Kim, S. S. Jang, H. Kyung, M. S. Kang, K. H. Lee and W. C. Yoo, *Adv. Funct. Mater.*, 2020, **30**, 1–11.

32 Y. Xie, H. Zhang, H. Huang, Z. Wang, Z. Xu, H. Zhao, Y. Wang, N. Chen and W. Yang, *Nano Energy*, 2020, **74**, 104928.

33 S. T. Senthilkumar, Y. Wang and H. Huang, *J. Mater. Chem. A*, 2015, **3**, 20863–20879.

34 Z. Xing, Q. Chu, X. Ren, J. Tian, A. M. Asiri, K. A. Alamry, A. O. Al-Youbi and X. Sun, *Electrochem. Commun.*, 2013, **32**, 9–13.

35 L. Manjakkal, C. G. Núñez, W. Dang and R. Dahiya, *Nano Energy*, 2018, **51**, 604–612.

36 J. Huang, K. Yuan and Y. Chen, *Adv. Funct. Mater.*, 2022, **32**, 1–68.

37 M. Ma, Z. Shi, Y. Li, Y. Yang, Y. Zhang, Y. Wu, H. Zhao and E. Xie, *J. Mater. Chem. A*, 2020, **8**, 4827–4835.

38 T. Gu and B. Wei, *J. Mater. Chem. A*, 2016, **4**, 12289–12295.

39 M. Yao, A. Liu, C. Xing, B. Li, S. Pan, J. Zhang, P. Su and H. Zhang, *Chem. Eng. J.*, 2020, **394**, 124883.

40 K. Wasnik, M. D. Pawar, L. R. Raphael, A. Pullanchiyodan, M. V. Shelke and P. Raghavan, *J. Mater. Res.*, 2022, **37**, 3865–3889.

41 A. Borenstein, O. Hanna, R. Attias, S. Luski, T. Brousse and D. Aurbach, *J. Mater. Chem. A*, 2017, **5**, 12653–12672.

42 S. Najib and E. Erdem, *Nanoscale Adv.*, 2019, **1**, 2817–2827.

43 N. Wu, X. Bai, D. Pan, B. Dong, R. Wei, N. Naik, R. R. Patil and Z. Guo, *Adv. Mater. Interfaces*, 2021, **8**, 1–17.

44 C. Q. Yi, J. P. Zou, H. Z. Yang and X. Leng, *Trans. Nonferrous Met. Soc. China*, 2018, **28**, 1980–2001.

45 V. Khomenko, E. Raymundo-Piñero, E. Frackowiak and F. Béguin, *Appl. Phys. A: Mater. Sci. Process.*, 2006, **82**, 567–573.

46 S. Jha, S. Mehta, Y. Chen, R. Likhari, W. Stewart, D. Parkinson and H. Liang, *Energy Storage*, 2020, **2**, 1–31.

47 K. Shi and K. P. Giapis, *ACS Appl. Energy Mater.*, 2018, **1**, 296–300.

48 O. Sadak, W. Wang, J. Guan, A. K. Sundramoorthy and S. Gunasekaran, *ACS Appl. Nano Mater.*, 2019, **2**, 4386–4394.

49 H. Yang, *Int. J. Electrochem. Sci.*, 2019, **14**, 7811–7831.

50 Q. Huang, L. Liu, D. Wang, J. Liu, Z. Huang and Z. Zheng, *J. Mater. Chem. A*, 2016, **4**, 6802–6808.

51 D. Gugulothu, A. Barhoum, R. Nerella, R. Ajmer and M. Bechelany, *Handbook of Nanofibers*, Springer International Publishing, 2019, pp. 45–77.

52 N. S. Jishnu, S. K. Vineeth, A. Das, N. T. M. Balakrishnan, A. P. Thomas, M. J. Jabeen Fatima, J. H. Ahn and R. Prasanth, *Materials Horizons: From Nature to Nanomaterials*, Springer Nature, 2021, pp. 201–234.

53 S. S. Ray, S. S. Chen, C. W. Li, N. C. Nguyen and H. T. Nguyen, *RSC Adv.*, 2016, **6**, 85495–85514.

54 A. Haider, S. Haider and I. K. Kang, *Arab. J. Chem.*, 2018, **11**, 1165–1188.

55 V. Beachley and X. Wen, *Mater. Sci. Eng., C*, 2009, **29**, 663–668.

56 B. Ghorani and N. Tucker, *Food Hydrocolloids*, 2015, **51**, 227–240.

57 A. Das, N. T. M. Balakrishnan, J. D. Joyner, N. Medhavi, O. Manaf, M. J. Jabeen Fatima, J.-H. Ahn, W. Ali and R. Prasanth, *Electrospinning: The State of Art Technique for the Production of Nanofibers and Nanofibrous Membranes for Advanced Engineering Applications*, Springer, Singapore, 2021, pp. 23–71.

58 X. Lu, C. Wang, F. Favier and N. Pinna, *Adv. Energy Mater.*, 2017, **7**, 1–43.

59 X. Liu, M. Naylor Marlow, S. J. Cooper, B. Song, X. Chen, N. P. Brandon and B. Wu, *J. Power Sources*, 2018, **384**, 264–269.

60 M. Mirjalili and S. Zohoori, *J. Nanostruct. Chem.*, 2016, **6**, 207–213.

61 J. Zhong, H. Zhang, J. Yan and X. Gong, *Colloids Surf., B*, 2015, **136**, 772–778.

62 O. Batnyam, S. I. Suye and S. Fujita, *RSC Adv.*, 2017, **7**, 51264–51271.

63 F. Pantò, Y. Fan, P. Frontera, S. Stelitano, E. Fazio, S. Patanè, M. Marelli, P. Antonucci, F. Neri, N. Pinna and S. Santangelo, *J. Electrochem. Soc.*, 2016, **163**, A2930–A2937.

64 B. Vidyadharan, I. I. Misnon, J. Ismail, M. M. Yusoff and R. Jose, *J. Alloys Compd.*, 2015, **633**, 22–30.

65 Y. Lee, S. Chae, H. Park, J. Kim and S. H. Jeong, *Chem. Eng. J.*, 2020, **382**, 122798, DOI: 10.1016/j.cej.2019.122798.

66 D. Zhang, J. Li, Z. Su, S. Hu, H. Li and Y. Yan, *J. Adv. Ceram.*, 2018, **7**, 246–255.

67 H. Shao, J. Fang, H. Wang and T. Lin, *RSC Adv.*, 2015, **5**, 14345–14350.

68 M. V. Vellayappan, J. R. Venugopal, S. Ramakrishna, S. Ray, A. F. Ismail, M. Mandal, A. Manikandan, S. Seal and S. K. Jaganathan, *RSC Adv.*, 2016, **6**, 83638–83655.

69 L. Manjakkal, A. Pullanchiyodan, N. Yogeswaran, E. S. Hosseini and R. Dahiya, *Adv. Mater.*, 2020, **32**(24), 1907254, DOI: 10.1002/adma.201907254.

70 Z. S. Iro, C. Subramani and S. S. Dash, *Int. J. Electrochem. Sci.*, 2016, **11**, 10628–10643.

71 S. Palchoudhury, K. Ramasamy, R. K. Gupta and A. Gupta, *Front. Mater.*, 2019, **5**, 1–9.

72 M. Cakici, K. R. Reddy and F. Alonso-Marroquin, *Chem. Eng. J.*, 2017, **309**, 151–158.

73 A. Das, A. Paul, N. Medhavi, N. T. M. Balakrishnan, M. A. Krishnan, J.-H. Ahn, J. Jabeen Fatima M and R. Prasanth, *Molybdenum Disulfide (MoS₂) and Its Nanocomposites as High-Performance Electrode Material for Supercapacitors*, Springer, Cham, 2021, pp. 59–90.

74 Y. Shao, M. F. El-Kady, J. Sun, Y. Li, Q. Zhang, M. Zhu, H. Wang, B. Dunn and R. B. Kaner, *Chem. Rev.*, 2018, **118**, 9233–9280.

75 P. Simon and Y. Gogotsi, *Nat. Mater.*, 2020, **19**, 1151–1163.

76 S. Zhai, H. E. Karahan, C. Wang, Z. Pei, L. Wei and Y. Chen, *Adv. Mater.*, 2020, **32**, 1–19.

77 A. B. Dalton, S. Collins, E. Muñoz, J. M. Razal, V. H. Ebron, J. P. Ferraris, J. N. Coleman, B. G. Kim and R. H. Baughman, *Nature*, 2003, **423**, 703.

78 J. Bae, M. K. Song, Y. J. Park, J. M. Kim, M. Liu and Z. L. Wang, *Angew. Chem., Int. Ed.*, 2011, **50**, 1683–1687.

79 Z. Yu, L. Tetard, L. Zhai and J. Thomas, *Energy Environ. Sci.*, 2015, **8**, 702–730.

80 J. Liang, H. Zhao, L. Yue, G. Fan, T. Li, S. Lu, G. Chen, S. Gao, A. M. Asiri and X. Sun, *J. Mater. Chem. A*, 2020, **8**, 16747–16789.

81 G. Zhu, H. Wen, M. Ma, W. Wang, L. Yang, L. Wang, X. Shi, X. Cheng, X. Sun and Y. Yao, *Chem. Commun.*, 2018, **54**, 10499–10502.

82 Y. Cao, J. Liang, X. Li, L. Yue, Q. Liu, S. Lu, A. M. Asiri, J. Hu, Y. Luo and X. Sun, *Chem. Commun.*, 2021, **57**, 2343–2355.

83 B. K. Balan, H. D. Chaudhari, U. K. Kharul and S. Kurungot, *RSC Adv.*, 2013, **3**, 2428–2436.

84 M. A. A. Mohd Abdah, N. H. N. Azman, S. Kulandaivalu and Y. Sulaiman, *Mater. Des.*, 2020, **186**, 108199.

85 D. Majumdar, T. Maiyalagan and Z. Jiang, *ChemElectroChem*, 2019, **6**, 4343–4372.

86 C. C. Hu, K. H. Chang, M. C. Lin and Y. T. Wu, *Nano Lett.*, 2006, **6**, 2690–2695.

87 M. Toupin, T. Brousse and D. Bélanger, *Chem. Mater.*, 2004, **16**, 3184–3190.

88 D. Wu, X. Xie, Y. Zhang, D. Zhang, W. Du, X. Zhang and B. Wang, *Front. Mater.*, 2020, **7**, 1–16.

89 N. Yu, H. Yin, W. Zhang, Y. Liu, Z. Tang and M. Q. Zhu, *Adv. Energy Mater.*, 2016, **6**, 1501458.

90 B. Xu, M. Zheng, H. Tang, Z. Chen, Y. Chi, L. Wang, L. Zhang, Y. Chen and H. Pang, *Nanotechnology*, 2019, **30**, 204002.

91 F. Shi, L. Li, X. L. Wang, C. D. Gu and J. P. Tu, *RSC Adv.*, 2014, **4**, 41910–41921.

92 D. Tian, C. Wang and X. Lu, *Adv. Energy Sustainability Res.*, 2021, **2**, 2100024.

93 G. Nie, X. Lu, M. Chi, M. Gao and C. Wang, *J. Colloid Interface Sci.*, 2018, **509**, 235–244.

94 D. Tian, N. Song, M. Zhong, X. Lu and C. Wang, *ACS Appl. Mater. Interfaces*, 2020, **12**, 1280–1291.

95 K. Xu, S. Li, J. Yang and J. Hu, *J. Colloid Interface Sci.*, 2018, **513**, 448–454.

96 X. Li, G. Wang, X. Wang, X. Li and J. Ji, *J. Mater. Chem. A*, 2013, **1**, 10103.

97 D. G. Lee and B. H. Kim, *Synth. Met.*, 2016, **219**, 115–123.

98 X. Sun, T. Xu, J. Bai and C. Li, *ACS Appl. Energy Mater.*, 2019, **2**, 8675–8684.

99 O. Pech and S. Maensiri, *J. Alloys Compd.*, 2019, **781**, 541–552.

100 B. H. Kim, C. H. Kim and D. G. Lee, *J. Electroanal. Chem.*, 2016, **760**, 64–70.

101 K. S. Yang, C. H. Kim and B. H. Kim, *Electrochim. Acta*, 2015, **174**, 290–296.

102 S. Jeon, J. H. Jeong, H. Yoo, H. K. Yu, B. H. Kim and M. H. Kim, *ACS Appl. Nano Mater.*, 2020, **3**, 3847–3858.

103 G. Binitha, M. S. Soumya, A. A. Madhavan, P. Praveen, A. Balakrishnan, K. R. V. Subramanian, M. V. Reddy, S. V. Nair, A. S. Nair and N. Sivakumar, *J. Mater. Chem. A*, 2013, **1**, 11698–11704.

104 C. T. Cherian, J. Sundaramurthy, M. Kalaivani, P. Ragupathy, P. S. Kumar, V. Thavasi, M. V. Reddy, C. H. Sow, S. G. Mhaisalkar, S. Ramakrishna and B. V. R. Chowdari, *J. Mater. Chem.*, 2012, **22**, 12198–12204.

105 X. Xia, Q. Hao, W. Lei, W. Wang, D. Sun and X. Wang, *J. Mater. Chem.*, 2012, **22**, 16844–16850.

106 X. Zhao, C. Johnston and P. S. Grant, *J. Mater. Chem.*, 2009, **19**, 8755–8760.

107 P. M. Kulal, D. P. Dubal, C. D. Lokhande and V. J. Fulari, *J. Alloys Compd.*, 2011, **509**, 2567–2571.

108 N. Iqbal, X. Wang, A. A. Babar, G. Zainab, J. Yu and B. Ding, *Sci. Rep.*, 2017, **7**, 1–10.

109 G. Nie, X. Lu, J. Lei, Z. Jiang and C. Wang, *J. Mater. Chem. A*, 2014, **2**, 15495–15501.

110 C. Ban, N. A. Chernova and M. S. Whittingham, *Electrochem. Commun.*, 2009, **11**, 522–525.

111 G. Wee, H. Z. Soh, Y. L. Cheah, S. G. Mhaisalkar and M. Srinivasan, *J. Mater. Chem.*, 2010, **20**, 6720–6725.

112 V. Aravindan, Y. L. Cheah, W. F. Mak, G. Wee, B. V. R. Chowdari and S. Madhavi, *ChemPlusChem*, 2012, **77**, 570–575.

113 R. Thangappan, S. Kalaiselvam, A. Elayaperumal and R. Jayavel, *Solid State Ionics*, 2014, **268**, 321–325.

114 S. Ding, T. Zhu, J. S. Chen, Z. Wang, C. Yuan and X. W. Lou, *J. Mater. Chem.*, 2011, **21**, 6602–6606.

115 C. Yuan, X. Zhang, L. Su, B. Gao and L. Shen, *J. Mater. Chem.*, 2009, **19**, 5772–5777.

116 M. S. Kolathodi, M. Palei and T. S. Natarajan, *J. Mater. Chem. A*, 2015, **3**, 7513–7522.

117 B. Vidhyadharan, N. K. M. Zain, I. I. Misnon, R. A. Aziz, J. Ismail, M. M. Yusoff and R. Jose, *J. Alloys Compd.*, 2014, **610**, 143–150.

118 M. Kundu and L. Liu, *Mater. Lett.*, 2015, **144**, 114–118.

119 Q. Li, J. Guo, D. Xu, J. Guo, X. Ou, Y. Hu, H. Qi and F. Yan, *Small*, 2018, **14**, 1704203.

120 F. Liu, H. Su, L. Jin, H. Zhang, X. Chu and W. Yang, *J. Colloid Interface Sci.*, 2017, **505**, 796–804.

121 T. Mukhiya, G. P. Ojha, B. Dahal, T. Kim, K. Chhetri, M. Lee, S. H. Chae, A. Muthurasu, A. P. Tiwari and H. Y. Kim, *ACS Appl. Energy Mater.*, 2020, **3**, 3435–3444.

122 T. Mukhiya, B. Dahal, G. P. Ojha, K. Chhetri, M. Lee, T. Kim, S. H. Chae, A. P. Tiwari, A. Muthurasu and H. Y. Kim, *Composites, Part B*, 2019, **178**, 107482.

123 B. Vidyadharan, R. A. Aziz, I. I. Misnon, G. M. Anil Kumar, J. Ismail, M. M. Yusoff and R. Jose, *J. Power Sources*, 2014, **270**, 526–535.

124 M. Kumar, A. Subramania and K. Balakrishnan, *Electrochim. Acta*, 2014, **149**, 152–158.

125 A. Mohammadpour-Haratbar, P. Kiaeerad, S. Mazinani, A. M. Bazargan and F. Sharif, *Ceram. Int.*, 2022, **48**, 10015–10023.

126 T. Wang, Y. Wang, J. Lei, K. Chen and H. Wang, *Exploration*, 2021, **1**, 20210178.

127 M. Kong, Z. Wang, W. Wang, M. Ma, D. Liu, S. Hao, R. Kong, G. Du, A. M. Asiri, Y. Yao and X. Sun, *Chem. – Eur. J.*, 2017, **23**, 4435–4441.

128 D. Tian, X. Lu, G. Nie, M. Gao and C. Wang, *Inorg. Chem. Front.*, 2018, **5**, 635–642.

129 G. Nie, X. Lu, M. Chi, Y. Zhu, Z. Yang, N. Song and C. Wang, *Electrochim. Acta*, 2017, **231**, 36–43.

130 B. Joshi, E. Samuel, Y. Kim, T. Kim, M. El-Newehy, A. Aldalbahi and S. S. Yoon, *Int. J. Energy Res.*, 2022, **46**, 22100–22112.

131 A. V. Radhamani, M. Krishna Surendra and M. S. Ramachandra Rao, *Mater. Des.*, 2018, **139**, 162–171.

132 L. Chang, C. Li, H. Ouyang, J. Huang, Q. Huang and Z. Xu, *Mater. Lett.*, 2019, **240**, 21–24.

133 H. Yu, H. Zhao, Y. Wu, B. Chen and J. Sun, *J. Phys. Chem. Solids*, 2020, **140**, 109385.

134 E. Samuel, A. Aldalbahi, M. El-Newehy, H. El-Hamshary and S. S. Yoon, *Ceram. Int.*, 2022, **48**, 18374–18383.